

1  
2  
3  
4  
5 1     **Arclogites and their role in continental evolution; Part 1:**  
6  
7 2     **Background, locations, petrography, geochemistry, chronology and**  
8  
9     **thermobarometry**  
10  
11 4  
12  
13 5  
14  
15 6  
16  
17 7  
18  
19 8  
20  
21 9

22  
23 10                   Mihai N. Ducea<sup>1,2</sup>

24 11                   Alan D. Chapman<sup>3</sup>

25 12                   Emilie Bowman<sup>1</sup>

26 13  
27 14  
28 15  
29 16  
30 17                   <sup>1</sup> University of Arizona, Tucson, AZ 85721, USA

31 18                   <sup>2</sup> Faculty of Geology and Geophysics, University of Bucharest, 010041, Bucharest, Romania

32 19                   <sup>3</sup> Geology Department, Macalester College, St. Paul, MN 55105, USA  
33 20  
34 21  
35 22  
36 23  
37 24  
38 25  
39 26  
40 27  
41 28  
42 29  
43 30  
44 31  
45 32  
46 33  
47 34  
48 35  
49 36  
50 37  
51 38  
52 39  
53 40  
54 41  
55 42  
56 43  
57 44  
58 45  
59 46  
60 47  
61 48  
62 49  
63 50  
64 51  
65 52

30 14                   **Abstract**

33 16     Arclogites, or clinopyroxene-, garnet-, amphibole-, and Fe-Ti oxide-bearing cumulates and restites  
34 17     (collectively representing residues) to andesitic continental arc magmas, are reviewed here and in  
35 18     a companion paper (Ducea et al., 2020). Experimental petrology and petrologic observations  
36 19     suggest that these eclogite facies rocks form magmatically in deep crustal hot zones beneath arcs  
37 20     with crustal thicknesses exceeding 35-40 km. Volcanic and plutonic products of thinner arcs may  
38 21     instead be entirely extracted from amphibolite to granulite facies and garnet-free pyroxenite  
39 22     residues. Arclogites are perhaps best known as xenoliths, with notable examples from young  
40 23     (Sierra Nevada and Central Arizona) and modern (Colombia) sub-arc environments. We suspect  
41 24     that arclogite occurs more commonly than currently recognized in the xenolith record from  
42 25     orogenic and cratonic domains. Arclogite is also found as discrete intervals in the deepest  
43 26     exposures of the Kohistan arc and as small volume inclusions in tectonically exposed peridotite  
44 27     massifs (e.g., Beni Bousera, Morocco). Geochemically, these rocks are low silica ( $\text{SiO}_2 < 50\%$ )  
45 28     assemblages with low Nb/Ta and Sr/Y ratios and enrichments in heavy REEs such that they  
46 29     represent the complement to the andesitic-dacitic liquids that make up the surface volcanics and  
47 30     batholiths of most arcs. Virtually all rock-forming minerals in arclogites are of similar or greater

density than the underlying mantle, making them ideal candidates for foundering. Arclogites are formed in the lowermost crust of arcs at 35-70 km depth and record high temperatures (~800-1000 °C) at the time of formation which then cool and metamorphose at ~650-750 °C if they remain attached to the crust for an extended period of time. Ages of these rocks are obtainable by Sm-Nd and Lu-Hf garnet isochron geochronology as well as titanite or rutile U-Pb geochronology, although these ages can be reset through long-term storage in hot lower crustal environments. Recent discovery of zircon accessory minerals in arclogites makes these rocks datable with greater precision and greater chance of preserving crystallization ages by U-Pb chronology.

Keywords: arclogite, arc roots, residues, cumulates, restites, thermobarometry, U-Pb zircon geochemistry

## **1. Introduction**

Sub-arc residual eclogite facies assemblages dominated by clinopyroxene-garnet-amphibole and iron-titanium oxides are together known as “arclogites”, a new term introduced to simplify the description of these rocks (Lee and Anderson, 2015). These rocks are cumulates and/or restites left behind by the fractionation/partial melting processes that produces the extensive intermediate melts found in both continental and oceanic arcs (Ducea and Saleeby, 1998a, Ducea, 2001, 2002). However, not all residual masses of large batholiths are arclogitic; thinner arcs are complemented by either plagioclase-rich cumulate sequences (Kay and Kay, 1985; Ducea et al., 2003) that survive in the geologic record as granulite terrains or as ultramafic masses dominated by garnet-free clinopyroxenites (Jagoutz, 2010, Jagoutz and Kelemen, 2015). Sub-arc garnet-free pyroxenites can founder in the mantle under certain circumstances (Jull and Kelemen, 2001), but when garnet is present, these residual masses are almost certain to return to the convective upper mantle due to their extreme negative buoyancy (Lee, 2014). Moreover, the more garnet and/or amphibole and iron oxides present in such assemblages, the higher the silica in the differentiated upper crust. Cumulates of pyroxene and plagioclase have silica concentrations similar to or higher than the bulk basaltic compositions of mantle-derived arc magmas, thus they alone cannot explain the diversification of magmatic arc liquid compositions toward intermediate and silicic values. It has

1  
2  
3  
4 62 thus been hypothesized that the formation of arclogite residues (restitute and cumulates) is an  
5  
6 63 important driver for making bulk continental crustal materials at subduction margins in modern  
7  
8 64 tectonic settings (Ducea, 2002). Similar assemblages could have also formed in the distant  
9  
10 65 geologic past, by remelting of thick basaltic keels at depths of tens of kilometers beneath the  
11  
12 66 surface; these basaltic protocontinents likely formed by processes other than subduction (Ernst,  
13  
14 67 2009).

15 68  
16  
17 69 Although continentalization and the driving of continental crust toward intermediate compositions  
18  
19 70 may rely on subduction-related arc magmatism (Gill, 1981, Taylor and McLemman, 1985, Stern,  
20  
21 71 2002, Davidson et al., 2007, Ducea et al., 2015, many others), the bulk composition of the  
22  
23 72 continental crust is also influenced by the formation and removal of low-silica arclogitic residues.  
24  
25 73 Yet relatively little is known about these arclogitic assemblages in nature. Rocks of arclogitic  
26  
27 74 composition are known as xenoliths from a few selected sub-arc locations worldwide and perhaps  
28  
29 75 also from the lowermost parts of exposed arc roots. Due to their deep origin and high density, these  
30  
31 76 assemblages are unlikely to be exhumed to the surface and preserved in the geologic record (see  
32  
33 77 discussion below). Nevertheless, their significance in magmatic and tectonic processes is  
34  
35 78 suggested by experimental petrologic results. Moreover, arclogites are the most likely candidates  
36  
37 79 to undergo foundering (*sensu lato*) because they are significantly denser than any other materials  
38  
39 80 hypothesized to engage in sub-crustal vertical tectonics, for which many names have been used in  
40  
41 81 the literature: dripping, delamination, convective removal, deblobbing (in the case of arc roots:  
42  
43 82 Kay and Kay, 1993, Ducea and Saleeby, 1998a, Ducea, 2002, Lee, 2014, Currie et al., 2015, Lee  
44  
45 83 and Anderson, 2015, in the more general sense: Arndt and Goldstein, 1989). From this perspective  
46  
47 84 alone, the details of arclogite petrology and geochemistry are of great significance not only to  
48  
49 85 subduction-centric arc petrologists but to continental tectonicists in general.

50 86  
51  
52 87 Below we review the main xenolith and tectonically exposed locations of these rocks, experimental  
53  
54 88 findings predicting their distribution under arcs at depth, and their petrography, thermobarometry,  
55  
56 89 chemical and isotopic characteristics, and ages. In a companion paper, we will review how  
57  
58 90 arclogites influence the major elemental composition of arcs, arclogite density and susceptibility  
59  
60 91 to convective removal, the composition of melts formed during their descent into the mantle, long-

1  
2  
3  
4 92 term arclogite production on Earth, and their long-term isotopic signatures once recycled into the  
5  
6 93 mantle.

7  
8 94  
9  
10 95 **2. Eclogites and arclogites**

11 96  
12  
13 97 Eclogites were defined as biminerally mafic rocks consisting of garnet and jadeitic clinopyroxene  
14  
15 98 (Hauy, 1822). It later became clear that these rocks represent high pressure assemblages, perhaps  
16  
17 99 at the highest end of plausible pressure conditions of crustal metamorphism. Through this  
18  
19 100 revelation, an “eclogite facies” was defined (Eskola, 1920), at first for mafic assemblages and then  
20  
21 101 for all other major chemical compositions. Due to its constituent minerals, the most salient feature  
22  
23 102 of a mafic eclogite is its high density. Garnet in particular is denser than most other common rock-  
24  
25 103 forming minerals. Eclogites represent a minuscule fraction of the known continental crust yet have  
26  
27 104 become a significant influencer of plate tectonics theory due to the realization that the oceanic  
28  
29 105 crust turns into eclogite upon subduction (Godard, 2001, for references and a view on history of  
30  
31 106 eclogite research). The negative buoyancy of any dense eclogite-facies subducting slab is a major  
32  
33 107 driver of plate tectonics.

34 108  
35 109 Consequently, eclogite has to a first order become synonymous in modern geology with a high  
36  
37 110 pressure metamorphic equivalent of basalt, and in particular, the subducting oceanic crust. Of  
38  
39 111 course, any composition other than mafic can become an eclogite facies rock if subjected to high  
40  
41 112 enough metamorphic pressures. These rocks would display the signature garnet and clinopyroxene  
42  
43 113 association among other phases stable in that assemblage at high pressure (Philpotts and Ague,  
44  
45 114 2009). Because eclogitic high-pressure equivalents of basalt typically have high clinopyroxene to  
46  
47 115 garnet ratios and contain jadeite-rich clinopyroxene, rocks that appear eclogitic but do not display  
48  
49 116 these characteristics have been referred to as garnet clinopyroxenites, ariegites, pyrigarnites, and  
50  
51 117 other names (Godard, 2001). As noted in a seminal paper (Coleman et al 1965), there are “eclogites  
52  
53 118 and eclogites” and that diversity is immediately obvious in their clinopyroxene as well as garnet  
54  
55 119 composition.

56 120  
57 121 A different type of eclogites, termed igneous eclogites, were first observed in the 19<sup>th</sup> century (e.g.  
58  
59 122 Holland, 1896). High pressure experimental work beginning in the 1960s later predicted that these

igneous eclogites form at high pressures as a result of fractionation of basalts at mantle depths (e.g. Green and Ringwood, 1967 a and b, Banno, 1970, Basaltic Volcanism Study Project, 1981). As a result, many eclogite assemblages found in the mantle, e.g. as xenoliths in kimberlites, were interpreted as primary igneous products (cumulates) rather than as pieces of slabs recycled in the mantle. Terminology is uneven here too, since eclogitic xenoliths in kimberlites are in some cases called pyroxenites and in others eclogites. Kimberlite eclogite literature is too vast and complex to review here (Jacob, 2004, Aulbach and Arndt, 2019 and references therein) and the origin of olivine-free, garnet-pyroxene xenoliths in such rocks is still debated. Without a doubt, however, these rocks were sampled from the lithospheric mantle at the time of entrainment in the host kimberlite. Some are true eclogites, others are garnet pyroxenites, yet they all formed in ancient tectonic environments from processes difficult to constrain due to lack of geologic context.

The presence of small bodies of cumulate-textured garnet pyroxenites within larger masses of peridotites in the classic “upper mantle” sections exposed tectonically in Europe and Northern Africa (Harz, Lherz, Beni Bousera) is also consistent with an igneous origin (Pearson et al., 1993). These are viewed as products of peridotite-melt interaction or as cumulates of basaltic melts (Obata, 1980). It has also been recently suggested that some of these rocks, which have metamorphic textures (El Atrassi et al., 2013), have the characteristics of arc root cumulates and are presumably small fragments of foundered bodies in the mantle (Gisy et al., 2011).

A new class of igneous eclogites, commonly referred to today as *arclogites* (Anderson, 2005; Lee and Anderson, 2015), represent arc root assemblages. These arclogites are the main subject of this contribution. Following Coleman et al. (1965), these rocks are Group B eclogites, and are found as xenoliths in subduction related magmatic arc regions (Mukhopadhyay, 1989, Ducea and Saleeby, 1996, Weber et al., 2002). They have cumulate/restite textures, have been documented to be cogenetic with arc rocks such as batholiths (Ducea and Saleeby, 1998b), and originate from 1.2 to over 3.0 GPa pressures (Mukhopadhyay, 1989, Ducea and Saleeby, 1996). Their discovery coincided with a series of new petrology experiments aimed at producing tonalites and granodiorites by dehydration melting of amphibolites (Rushmer, 1991, Wolf and Wyllie, 1993, 1994, Rapp and Watson, 1995). These experiments noted that at pressures in excess of 1 GPa, abundant garnet forms in equilibrium with intermediate melts. With a better understanding of the

1  
2  
3  
4 154 roles of plagioclase, pyroxene, garnet, and amphibole fractionation in intermediate melts at deep  
5  
6 155 crustal levels in thick arcs (the so-called MASH zones, Hildreth and Moorbath, 1988, or hot zones,  
7  
8 156 Annen et al., 2006), a leading hypothesis emerged that these eclogite-like igneous assemblages  
9  
10 157 may dominate the roots of thick arcs at lower crustal levels and may be the main complement at  
11  
12 158 depth to near-surface batholiths or thick Andean-like volcanic arcs. The high density of such  
13  
14 159 assemblages also made them likely candidates for detachment and foundering into the mantle  
15  
16 160 (Ducea and Saleeby, 1998a), which can be entertained as a hypothesis for continental evolution  
17  
18 161 toward a more silicic crust (Rudnick, 1995, Ducea, 2002). These rocks, which often contain  
19  
20 162 amphibole in addition to pyroxenes and garnet, were referred to as eclogite (Dodge et al, 1986,  
21  
22 163 1988), garnet pyroxenites (Mukhopadhyay, 1989, Ducea and Saleeby, 1996), low Mg-pyroxenites  
23  
24 164 (Lee et al., 2006), garnet-pyroxene-amphibole rocks (Smith et al., 1994), pyribolites, pyroxenites,  
25  
26 165 pyrigarnites (Weber et al., 2002), “arc-eclogites” (Anderson, 2005), and eventually arclogites (Lee  
27  
28 166 and Anderson, 2015).

29  
30 168 Note that in contrast to Lee and Anderson (2015), we do not include in the umbrella term  
31  
32 169 “arclogite” the so-called high-Mg pyroxenites, which are garnet websterites found in virtually all  
33  
34 170 arclogite locations described below. In contrast to the low-Mg pyroxenites (garnet  
35  
36 171 clinopyroxenites), which are actually arclogites, garnet websterites equilibrated at higher pressures  
37  
38 172 that are indubitably located within the mantle (2.5 GPa or more) and are more likely former mafic  
39  
40 173 melts (not residues) frozen in the uppermost mantle. These rocks are in our view spatially  
41  
42 174 associated with peridotites as veins within the subcontinental lithospheric mantle, whereas the  
43  
44 175 arclogites are true deep residues of the arcs, straddling the complex boundary between the crust  
45  
46 176 and mantle in supra-subduction environments and transitioning at shallower depths to granulite  
47  
48 177 assemblages.

### 49 50 179 **3. Locations**

51  
52 180  
53  
54 181 Our main source of information regarding arclogites comes from xenoliths entrained in volcanic  
55  
56 182 rocks sampling sub-continental arc domains. In addition, there exist some xenolith localities in the  
57  
58 183 thin oceanic arcs of the Circum-Pacific (Conrad and Kay, 1984, Kay and Kay, 1985; DeBari et al.,  
59  
60 184 1987, McInnes et al., 2001), but these xenoliths do not contain arclogitic assemblages. They do  
61  
62  
63  
64  
65

1  
2  
3  
4 185 however contain garnet-free pyroxenites, wehrlites, and other garnet-free ultramafites which could  
5  
6 186 make up the dense roots of island arcs (as envisioned in the theoretical study of Jull and Kelemen,  
7  
8 187 2001).

9  
10 188  
11 189 The main North American xenolith arclogite localities are in the central Sierra Nevada, California  
12  
13 190 (Domenick et al., 1983, Dodge et al., 1986,1988, Ducea and Saleeby, 1996, 1998a, b, c,  
14  
15 191 Mukhopadhyay, 1989, Mukhopadhyay and Manton, 1994, Lee et al., 2000, 2001a and b, 2006)  
16  
17 192 and central Arizona (Arculus and Smith, 1979, Esperanca et al., 1988, Chin et al, 2012, Chapman  
18  
19 193 et al., 2019, 2020, Rautela et al., 2020), and possibly include some of the sub-Colorado Plateau  
20  
21 194 xenolith localities. In South America, arclogites are known from one notable locality, Mercaderes  
22  
23 195 in southern Colombia (Webber et al., 2002, Bloch et al, 2017), which is the only known arclogite  
24  
25 196 xenolith locality from an active Andean-type arc. Similar rocks may be present in Miocene  
26  
27 197 volcanics from the western shores of Lake Titicaca (Chapman et al., 2015) but they have not been  
28  
29 198 studied in detail.

30 199  
31  
32 200 All known arclogite xenoliths are entrained within trachyandesitic, latitic, or other intermediate  
33  
34 201 volcanic material. This is in contrast to peridotite xenoliths, which are commonly hosted by  
35  
36 202 basaltic rocks (Nixon, 1987). Another common feature within these xenolith localities is the  
37  
38 203 abundance of xenoliths of many different lithologies, ranging from arclogites to igneous granulites,  
39  
40 204 metasedimentary granulite facies rocks, garnet-free clinopyroxenites, high-pressure garnet  
41  
42 205 websterites, and garnet ( $\pm$  spinel) peridotites. As is commonly the case with xenoliths, secondary  
43  
44 206 breakdown of some phases occurred during their entrainment in the host magma; for example,  
45  
46 207 kelyphitic rims on garnet are ubiquitous.

47 208  
48 209 Sierra Nevada arclogite xenolith localities include 8-12 Ma trachyandesite plugs that intruded the  
49  
50 210 Sierra Nevada batholith long after its demise (80 Ma). These are small volume exposures, the most  
51  
52 211 extensively studied of which are located at Pick and Shovel Mine, Chinese Peak, and near the town  
53  
54 212 of Big Creek, California (Domenick et al., 1983, Dodge et al., 1986, 1988, Mukhopadhyay, 1989,  
55  
56 213 Mukhopadhyay and Manton, 1994, Ducea and Saleeby, 1996, 1998a and b, Ducea, 2002, Lee et  
57  
58 214 al., 2000, 2001 a and b, 2006, Chin et al., 2012). A number of other small localities in the same  
59  
60 215 region have not been investigated (Ducea and Saleeby, 1996). The Sierra Nevada localities are

particularly instructive because the variety of mineral assemblages within the xenoliths allows construction of a cross section through the lithosphere (Saleeby et al., 2003, Figure 1). Younger (3-4 Ma) xenolith-bearing mafic lavas from the same area in the central Sierra Nevada do not contain any arc root xenoliths; they are much hotter and dominated by spinel peridotites (Ducea and Saleeby, 1996). This has led various authors to suggest that the sub-central Sierra arc root was delaminated at some point during the Pliocene (Ducea and Saleeby, 1996, 1998a, Farmer et al., 2002). In fact, the existence today of a high density (“eclogitic”) anomaly in the mantle beneath the south-central Sierra Nevada as revealed by seismic tomography data has been proposed to represent the delaminated (or foundered) body (Zandt et al., 2004, Jones et al., 2014).

Sierra Nevada arclogites range from garnetites to garnet clinopyroxenites with or without amphibole and Fe-Ti oxides. There are also cumulate rocks with alternating layers of garnet clinopyroxenite and plagioclase (Ducea and Saleeby, 1996), suggesting that a transition from plagioclase-bearing to plagioclase-free assemblages existed in the root of the arc. In addition, hornblende is present in at least half of all known arclogites. Many clinopyroxene grains in these rocks have amphibole cleavages, which suggests clinopyroxene formation as a result of amphibole dehydration. Garnet-free clinopyroxenites with abundant (up to 50%) magnetite-ilmenite are also rather abundant. Garnet peridotites are rare but are among the very few samples of the mantle lithosphere underlying western Cordilleran magmatic arcs (Mukhopadhyay and Manton, 1994, Lee et al., 2000, 2001a). Furthermore, garnet websterites are distinct from arclogites in that they are much more magnesian (Mukhopadhyay and Manton, 1994, Lee et al., 2006, Chin et al., 2012, 2014) and yield significantly higher equilibration pressures (on average ~1 GPa greater than arclogite). As such, garnet websterites are thought to represent fragments of the lithospheric mantle that reside much deeper than the arclogite-bearing near-Moho region.

The central Arizona xenolith localities are hosted by late Oligocene latites (Arculus and Smith, 1979, Esperanca et al., 1988, 1997, Smith et al., 1994, Erdman et al., 2016, Chapman et al. 2020). The best studied localities are Camp Creek and Chino Valley (see Chapman et al., 2019, for a field guide describing locations). Xenolithic rocks are very similar to those of the Sierra Nevada and range in composition from metasedimentary and metaigneous xenoliths representing the local basement to garnet granulites, garnet websterites, garnet-free peridotites, and recently recognized



arclogites (Erdman et al., 2016). Arclogites in this locality have been shown to be roots of the southern California arc displaced eastward (Rautela et al., 2020, Chapman et al., 2020) by ultra-shallow subduction along the Laramide corridor (Saleeby, 2003, Ducea and Chapman, 2018).

The Mercaderes xenolith locality (hosted by the Granatifera Tuff) in southern Colombia is a small presumed Quaternary sequence of satellite eruptions to the greater Dona Juana stratovolcano (Weber et al., 2002). Beneath this locality, the depth to seismic Moho is around 50-60 km (Bloch et al., 2017), although global seismic databases (Laske et al., 2013) shows it closer to 40-45 km. Like the North American localities, the Granatifera Tuffs, which are a sequence of tuffs and lahars, are intermediate in composition (andesites and lamprophyres, Rodriguez-Vargas et al., 2005) and host a variety of xenoliths ranging from volcanic, metasedimentary, granulite, pyroxenite (with and without garnet), garnet-bearing peridotite, to other more exotic assemblages (Rodriguez-Vargas et al., 2005). Based on their age and high recorded temperatures, the latter of which is which is unique among documented arclogitic localities, these rocks are inferred to represent fragments of a residual root formed by the 10-5 Ma arc magmatism that resulted in the buildup of the Dona Juana stratovolcano (Bloch et al., 2017).

A reexamination of published xenolith studies indicates that other possible arclogitic xenoliths exist elsewhere on the planet given their petrographic composition, although they have not been identified as such in the literature and await further study. A good example is the wealth of eclogite-like xenoliths with seemingly arclogitic characteristics found in SE Australia in small-scale Holocene volcanic rocks from western Victoria within the greater Lachlan Fold Belt province (Griffin and O'Reilly, 1986). However, no studies to date have interpreted those eclogite xenoliths as arc root assemblages. Another, albeit less convincing example of arclogite xenoliths is from the North China Craton (Gao et al., 2004, Lee, 2014).

Most ancient segments of the North, Central and South American Cordilleran arcs are exposed to relatively shallow levels (Ducea et al., 2015) less than 10 km on average. Few tectonic windows exist into deeper, usually no more than 30 km paleodepths (Ducea et al., 2015 for a review) that are not quite deep enough to represent the realm of plagioclase-free cumulates. In deeply exhumed arc sections of the North American Cordillera (e.g., the North Cascades, Salinian Block, and

1  
2  
3  
4 278 Tehachapi Mountains, all of which yield 0.8-1.0 GPa paleo-pressures), peritectic garnet textures  
5  
6 279 are observed in migmatitic amphibolite-bearing mafic rocks (e.g., Whitney, 1992; Pickett and  
7  
8 280 Saleeby, 1993; Wernicke and Getty, 1997; Kidder et al., 2003). However, these rocks are still  
9  
10 281 dominated by plagioclase. In other deep crustal arc sections, such as the Sierra Valle Fertil  
11  
12 282 (Otamendi et al., 2009, 2012), garnet is not present even in the deepest exposures (Walker et al.,  
13  
14 283 2015). One notable exception to the lack of arclogites in outcrop is the Kohistan arc (Pakistan),  
15  
16 284 which preserves an extraordinary cross-sectional view of a transitional island arc down to  
17  
18 285 paleodepths of over 30 km (Dhuime et al., 2009). Within the Kohistan arc, garnet-rich rocks  
19  
20 286 include rare exposures that could be categorized as arclogites.

21 287  
22  
23 288 The Kohistan paleo-island arc complex is sandwiched between India and Asia proper (Burg et al.,  
24  
25 289 1998) and is believed to have formed above an oceanic subduction zone within the Neotethys  
26  
27 290 between 117 and 85 Ma (Dhuime et al., 2009). Exposures include arc volcanics in the north and  
28  
29 291 the Kohistan batholith farther south. Southernmost exposures are best described along the Indus  
30  
31 292 river and contain units that represent the root of the arc (Zellinger, 2002 and Garrido et al., 2006,  
32  
33 293 and references therein). The deepest complex of the Kohistan arc, the Jijal complex (Jan and  
34  
35 294 Howie, 1981, Burg et al., 1998), is believed to expose the paleo-Moho of the arc due to the  
36  
37 295 presence of >1 GPa rocks that equilibrated at probably no more than 35 km paleodepths  
38  
39 296 (Yamamoto and Nakanura, 1996, 2000; Anczkiewicz and Vance, 2000). The Jijal complex  
40  
41 297 consists of a 3 km-thick section of garnet granulites and garnet gabbros, below which the section  
42  
43 298 transitions to olivine-rich ultramafic rocks (spinel peridotites) that represent the paleo-upper  
44  
45 299 mantle. At outcrop scale, the garnet granulite section does show transitions toward arclogitic  
46  
47 300 assemblages, including garnet-clinopyroxene-amphibole assemblages with various modal  
48  
49 301 proportions of these three minerals (Dhuime et al., 2009). The presence of arclogites that record  
50  
51 302 35 km paleodepths is consistent with experimental results, which predict the stabilization of  
52  
53 303 arclogite assemblages at these depths.

#### 54 304 55 305 **4. Experimental results**

56 306  
57 307 Dehydration melting experiments of wet basalts (amphibole-bearing gabbros or amphibolites) at  
58  
59 308 pressures over 1 GPa have shown convincingly that amphibole dehydration melting reactions

1  
2  
3  
4 309 produce intermediate compositions similar to the tonalites and granodiorites of modern  
5  
6 310 subduction-related arcs (Rushmer, 1991, Wolf and Wyllie, 1993, 1994, Rapp and Watson, 1995)  
7  
8 311 or that tonalitic liquids are in equilibrium with such assemblages (Carroll and Wyllie, 1990). These  
9  
10 312 experiments provide the foundation for understanding melting reactions along with the solid  
11  
12 313 phases present in equilibrium with realistic melting fractions in young lowermost orogenic crust  
13  
14 314 or some ancient thickened oceanic plateau-like crust (10-50%). Likewise, these experiments  
15  
16 315 provide an excellent framework for understanding the “second stage” process that occurs in the  
17  
18 316 lower crust of arcs, which is required for generating intermediate rocks (Dufek and Bergantz, 2005,  
19  
20 317 Jagoutz, 2014, Ducea et al., 2015). Although these experiments simulate partial melting, one can  
21  
22 318 think of running them down temperature in order to view the results as products of fractionation  
23  
24 319 in deep-crustal hot zone magma chambers. Amphibole is a key phase undergoing melting in these  
25  
26 320 experiments and provides the water for calc-alkaline intermediate melts. Fundamentally, these  
27  
28 321 classes of experiments can be viewed simply as amphibole dehydration melting reactions, which  
29  
30 322 take place at higher temperatures (850-950 °C) than muscovite and biotite dehydration reactions.  
31  
32 323 The main phases in equilibrium with tonalitic and granodioritic melts are plagioclase and  
33  
34 324 clinopyroxene. At higher pressures, plagioclase is replaced by garnet, leading the way to an  
35  
36 325 igneous “eclogitic” (arclogitic) assemblage at pressures in excess of 1.5 GPa. These experiments  
37  
38 326 show that garnet pyroxenite assemblages are not only expected to be in equilibrium with basaltic  
39  
40 327 melts at mantle pressures (Green and Ringwood, 1967 a and b) but also in intermediate and silicic  
41  
42 328 melts (Carroll and Wyllie, 1990). Amphibole remains on the liquidus if not entirely consumed by  
43  
44 329 the melting reaction but can also crystallize from fractions of melt left unextracted from the source  
45  
46 330 (or magma chamber). The gradual disappearance of plagioclase in favor of garnet with depth is  
47  
48 331 predicted to take place over a large range of pressures between 1 and 2 GPa and depends on the  
49  
50 332 bulk composition of the system. Therefore, these experiments reveal that the transition from  
51  
52 333 plagioclase-only to garnet-only assemblages within the deep crust of arcs is most likely not sharp,  
53  
54 334 and instead occurs gradually in the depth region of 35-50 km.

55  
56 335  
57 336 Figure 2 shows pMELTS-predicted (Ghiorso and Sack, 1995) assemblages on the liquidus of a  
58  
59 337 tonalitic melt for a bulk basaltic calc-alkaline composition (Schmidt and Jagoutz, 2017)  
60  
61 338 undergoing dehydration melting at 1 and 2 GPa respectively as a function of partial melt fraction.  
62  
63 339 The composition of garnet is shown in Figure 3 in the classic Coleman et al. (1965) garnet  
64  
65

1  
2  
3  
4 340 classification diagram. Note that the garnets predicted to form in these conditions are  
5  
6 341 predominantly almandinic (Group B of Coleman et al., 1965). Almandine-bearing arclogites are  
7  
8 342 significantly denser than eclogites from subducting environments (which contain Group C  
9  
10 343 garnets), mainly because these group B garnets are more Fe-rich and are also more abundant in  
11  
12 344 the rocks (see Section 5). These simple forward models anchored in vast amounts of experimental  
13  
14 345 data illustrate the predicted minerals that are expected to play a role in the differentiation of  
15  
16 346 granitoid magmas at depth.

## 17 347

### 18 348 5. Petrography

19 349

20  
21 349 Petrographically, arclogites globally are very similar; consequently, we will describe them as a  
22  
23 350 group and mention specific localities only when a feature stands out at that locale. These rocks are  
24  
25 351 relatively coarse-grained (typically  $1 \pm 0.5$  cm in diameter although finer equivalents exist) and  
26  
27 352 commonly exhibit cumulate textures with the two main phases (clinopyroxene and garnet)  
28  
29 353 displaying orthocumulate features. Almost all arclogitic xenoliths contain breakdown products  
30  
31 354 most clearly visible around garnets; these are known as kelyphitic rims which consist of very fine  
32  
33 355 assemblages of plagioclase, spinels, aluminous pyroxenes, and silicate glass. These features are  
34  
35 356 generally interpreted to represent breakdown reactions in the host magma carrying the xenolith  
36  
37 357 and do not have any pre-entrapment geologic significance. In addition to garnet and  
38  
39 358 clinopyroxene, relatively common minerals within arclogitic assemblages include pargasitic  
40  
41 359 amphibole, phlogopite, rutile, Fe-Ti oxides (magnetite, ilmenite, pseudobrookite), and  
42  
43 360 orthopyroxene (sometimes as exsolution lamellae in clinopyroxene). Of these phases, amphibole  
44  
45 361 and Fe-Ti oxides are the most abundant and can make up as much as 50% of the rock volume. The  
46  
47 362 difficulty of assigning a common name to these rocks arises from the fact that due to the small size  
48  
49 363 of xenoliths and large grainsize of constituent minerals, only portions of the rock may be exposed.  
50  
51 364 As a result, in some cases, true arclogites may be labeled as garnetites (with minor clinopyroxene  
52  
53 365 and amphibole), while others may be dominated by clinopyroxene or amphibole (Smith et al., 1994  
54  
55 366 named them “pyroxene-garnet-amphibole” rocks, recognizing their common lineage). Apatite is  
56  
57 367 also present in some arclogites, as are titanite, aluminous spinel, Cu-Fe sulfides, and zircon,  
58  
59 368 although these are all accessory phases never exceeding 1% by volume. Interestingly, native gold  
60  
61  
62  
63  
64  
65

1  
2  
3  
4 370 has been found in an arclogitic xenolith from Chino Valley in central Arizona (Arculus and Smith,  
5  
6 371 1979).

7  
8 372  
9  
10 373 Many clinopyroxenes have relic amphibole cleavages suggesting that these rocks record the  
11  
12 374 dehydration melting of amphibolites (Ducea and Saleeby, 1996). However, the opposite is also  
13  
14 375 recorded: some amphiboles display a pyroxene-like orthogonal cleavage, suggesting that some of  
15  
16 376 these amphiboles are secondary and come about due to hydration of the nominally anhydrous  
17  
18 377 garnet-clinopyroxene assemblage (Rautela et al., 2020). In arclogites, amphiboles are reactants in  
19  
20 378 some occurrences and reaction products in others.

21 379  
22  
23 380 Garnets are typically the most euhedral of phases and also contain the largest amounts of  
24  
25 381 inclusions. When they are not transformed to secondary phases, they are orange red in hand  
26  
27 382 specimen. Acicular rutile, zircon, apatite, and titanites are most commonly found as inclusions in  
28  
29 383 garnets, which may also contain more minor inclusions of clino- and orthopyroxenes. Garnets fall  
30  
31 384 in the middle of the Group B field of Coleman et al. (1965); they have more or less equal  
32  
33 385 proportions of almandine-pyrope and grossular, and if one end member does dominate, it is the  
34  
35 386 almandinic term. Cooled arclogites such as those from the Sierra Nevada and central Arizona  
36  
37 387 exhibit clear diffusional profiles (Ducea and Saleeby, 1996) and diffusionally modified growth  
38  
39 388 zonation (Rautela et al., 2020), respectively. In contrast, recently formed arclogites from  
40  
41 389 Mercaderes display flat major element profiles (Bloch et al., 2017). Kelyphitic rims are common  
42  
43 390 to all arclogite garnet samples.

44  
45 391  
46  
47 392 Clinopyroxenes are the most abundant of all arclogite phases and probably make up ~50% of these  
48  
49 393 rocks by volume on average. Most clinopyroxenes are salites and augites in composition. This is  
50  
51 394 consistent with the composition of arclogitic garnets, which also comprise roughly equal amounts  
52  
53 395 of the Mg, Fe, and Ca end members. Some rare jadeitic clinopyroxenes as well as grosspyditic  
54  
55 396 varieties were described from the Sierra Nevada localities (Domenick et al., 1983). Grosspyditic  
56  
57 397 clinopyroxenes are green to black when not altered, while the rarer jadeitic clinopyroxenes found  
58  
59 398 at all localities appear bright green. Orthopyroxenes occur as exsolution lamellae in clinopyroxene  
60  
61 399 and/or as small anhedral intercumulus phases together with clinopyroxenes. In some Sierra Nevada  
62  
63 400 arclogites, orthopyroxene occurs as small inclusions in garnet (Ducea and Saleeby, 1996). While  
64  
65

1  
2  
3  
4 401 orthopyroxene is merely an accessory phase in arclogites and does not occur in many of these  
5  
6 402 rocks, its presence is important in determining the pressure of equilibration of the assemblage.  
7

8 403  
9  
10 404 Amphiboles are ferroan pargasitic hornblendes and may be an absent or dominant phase in  
11  
12 405 arclogites, although in most cases they do not comprise more than 20% of the rock. Many  
13  
14 406 amphiboles have a relatively high concentration of Ti, which gives them a yellow brownish color  
15  
16 407 in hand specimen.  
17

18 408  
19 409 Fe-Ti oxides are rather common in arclogites, although they remain the least investigated mineral  
20  
21 410 at all localities. Magnetite, ilmenite, and rutile are most commonly described. While magnetite and  
22  
23 411 ilmenite can occur as large cumulate crystals that make up as much as 30-40% of some arclogites,  
24  
25 412 rutile is typically found as inclusions within garnet. Some garnet-free arclogites (clinopyroxenites),  
26  
27 413 especially those from the Chinese Peak locality in the Sierra Nevada, have up to 50% titanium  
28  
29 414 magnetites and form distinct layers at the scale of the thin section (Ducea and Saleeby, 1996).  
30

31 415  
32 416 While plagioclase is not a common phase in arclogites, transitions from arclogite to layered  
33  
34 417 granulite are observed in Sierra Nevada (Dodge et al., 1986), central Arizona (Esperanca et al.,  
35  
36 418 1988), and Mercaderes collections (Weber et al., 2002). In addition, small inclusions of plagioclase  
37  
38 419 are found in garnets at all locations. They have compositions ranging from oligoclase to andesine  
39  
40 420 and average out near the boundary between the two among all locations.  
41

42 421  
43 422 Phlogopite is an accessory mineral found in some hydrated arclogites along with amphibole at all  
44  
45 423 locations. Phlogopite rarely makes up more than 0.5% of the rock volume and is characterized by  
46  
47 424 high Ti content (up to 5%). Scapolite is a rare accessory mineral in arclogites and is typically a  
48  
49 425 sulfate-rich mizzonite (Weber et al., 2002). Apatite is included in garnets and is a fluorapatite with  
50  
51 426 a more minor hydroxyl component. Zircon, titanite, monazite and clinozoizite, when present, are  
52  
53 427 included in garnets. Chalcopyrite and other rare arclogitic minerals are not described further here.  
54

## 55 429 **6. Cumulates or restites?**

56 430  
57  
58  
59  
60  
61  
62  
63  
64  
65

1  
2  
3  
4 431 The cumulate versus restite origin of arclogitic assemblages has been extensively debated (Lee et  
5  
6 432 al., 2006, Jagoutz, 2014, Bloch et al., 2017). Geochemically, there is no clear way to uniquely  
7  
8 433 distinguish between a restite and cumulate origin by studying magmas that were extracted upwards  
9  
10 434 into the volcanic arc or subvolcanic batholith (Ducea et al., 2015). Petrographically, most of these  
11  
12 435 rocks have cumulate textures (Figure 4) and thus they are probably collections of minerals that  
13  
14 436 fractionated and separated within magma chamber environments *sensu lato*. However, the most  
15  
16 437 likely ratio of arc to residue in these environments is 1:1 to 1:3 (Ducea, 2002), meaning that if  
17  
18 438 these assemblages were restites of partial melting at high melt fraction, cumulate textures would  
19  
20 439 probably form anyway. One clear conclusion from Sierra Nevada and central Arizona localities is  
21  
22 440 that pre-existing lower crust was involved in the mass budget of the batholith (Ducea and Barton,  
23  
24 441 2007), which is evident in the radiogenic and stable isotopes of the arclogites (Esperança et al.,  
25  
26 442 1988; Smith et al., 1994; Ducea, 2002) and the presence of inherited Precambrian zircon grains  
27  
28 443 contained within them (Murphy and Chapman, 2018). This incorporation of the local lowermost  
29  
30 444 crust rules out a closed system fractionation environment. Altogether, the study of arclogites has  
31  
32 445 not at present sufficiently resolved the debate regarding cumulate versus restite origin, which has  
33  
34 446 implications for how hot zones (Annen et al., 2006) (or MASH zones, Hildreth and Moorbath,  
35  
36 447 1988) form under long-lived arcs and what they may look like in detail. Without a doubt, hot zones  
37  
38 448 are areas where partial melt resides for a long time (possibly millions of years) with heat constantly  
39  
40 449 added through intrusions of mantle-derived magma (Dufek and Bergantz, 2005, Annen et al. 2006)  
41  
42 450 over large areas (Ward et al., 2017, Delph et al., 2017). At high melt fraction in these solid-liquid  
43  
44 451 systems, searching for the difference between a cumulate and a restite may prove futile.

## 45 7. Geochemistry

46 452  
47  
48 453 Because most arclogites occur as cumulate-textured xenoliths that are 10-20 cm in diameter and  
49  
50 454 consist of relatively large minerals, they are inherently potentially unrepresentative. For this  
51  
52 455 reason, it is difficult to determine the average mineral abundance or bulk chemistry of arclogites.  
53  
54 456 Nevertheless, efforts to average various compositions have been made by various researchers (e.g.  
55  
56 457 Ducea, 2002, Lee, 2014). Average mineralogy or chemistry aside, a number of important features  
57  
58 458 of these rocks do stand out: (1) they are high-Fe, low-Mg eclogitic rocks, (2) contain little to no  
59  
60 459 orthopyroxene, (3) have a larger fraction of garnet than oceanic eclogites, averaging ~50% by  
61  
62  
63  
64  
65

462 volume, (4) are rich in Fe-Ti oxides (magnetite, ilmenite, and rutile), (5) have a variety of other  
463 accessory minerals such as zircon, apatite, and titanite, and (6) are not quartz normative.

464  
465 These common threads among all arclogites helped researchers estimate their average  
466 composition. Arclogites are anomalously low silica, which makes them ideal candidates for  
467 residues of intermediate melts. Consistent with this interpretation are the high FeO, and TiO<sub>2</sub>,  
468 which reflects differentiation toward intermediate melts envisioned by many to produce a trend  
469 like that shown in Figure 5 (from Lee et al., 2006). If there is no involvement (assimilation) of pre-  
470 existing intermediate crust, an average arc basalt requires roughly one-part average continental arc  
471 and two to three parts arclogite (Ducea, 2002; Ducea et al., 2015). If pre-existing continental crust  
472 is incorporated during partial melt residence in hot zones of the lowermost crust, the ratio of  
473 granitoid to arclogite decreases toward 1:1. Furthermore, the range of crystallization pressures in  
474 Sierra Nevada arclogites is consistent with a 1:1.5 ratio between batholith and residue (Ducea and  
475 Saleeby, 1996, Saleeby et al., 2003).

476  
477 Arclogites are enriched in heavy REE (Chin et al., 2014) due to their affinity for garnet, amphibole,  
478 and clinopyroxene. They are also enriched in HFSE such as Nb and Ta (Tang et al., 2019),  
479 providing a reservoir for storage of these elements depleted in arc magmas. An average REE  
480 profile of Sierra Nevada arclogites shows they are overall great complements of the upper- to mid-  
481 crustal batholith (Ducea, 2002; Figure 6).

482  
483 One of the debated aspects of the chemical evolution of the Earth is the imbalance of the Nb/Ta  
484 ratio in major continent-forming reservoirs – the Nb/Ta ratio is sub-chondritic (~19) in the crust  
485 and the depleted mantle (Rudnick et al., 2000). The missing high Nb/Ta reservoir was proposed to  
486 be some rutile-bearing eclogite from studies of kimberlitic eclogites, which are interpreted to be  
487 recycled oceanic crust (Rudnick et al., 2000). A more convincing explanation providing a direct  
488 link to continental formation was provided by Tang et al. (2019), who noted that rutile-bearing  
489 arclogites from central Arizona have high Nb/Ta ratios. Similarly, high Nb/Ta ratios have been  
490 measured within arclogites of the Sierra Nevada. These highly heterogeneous Nb/Ta ratios range  
491 from 20 to over 100 (Ducea, 2002) and are suggested to result from rutile, a high Nb/Ta phase  
492 abundant in arclogites (Tang et al., 2019) as inclusions within garnet. Additionally, ilmenite may



1  
2  
3  
4 493 have high Nb/Ta ratios, but this has yet to be precisely quantified. Because oceanic eclogites  
5  
6 494 (Group C) do not typically contain rutile (Coleman et al., 1965), arclogites are the most likely  
7  
8 495 reservoir to balance out the sub-chondritic Nb/Ta of the crust and depleted mantle.  
9

10 496  
11 497 Radiogenic isotopes, such as Sr, Nd, and Pb, of the Sierra Nevada arclogites have been studied in  
12  
13 498 detail at the whole-rock scale (Domenick et al., 1983, Ducea, 2001, 2002). On average, the isotopic  
14  
15 499 signatures of these arclogites, as well as their ages, are identical to those of the Dinkey Creek  
16  
17 500 intrusive suite, which makes up the surface geology of the central Sierra Nevada (Kistler, 1990).  
18  
19 501 Similarly, whole-rock isotopic values determined from central Arizona arclogite xenoliths overlap  
20  
21 502 those of Mojave Desert plutons, the inferred original (i.e., pre-shallow-angle subduction) location  
22  
23 503 of central Arizona arclogite (Esperanca et al., 1988, 1997; Smith et al., 1994; Rautela et al., 2020).  
24  
25 504 As such, both California and Arizona xenolithic arclogites are suspected to be petrogenetically  
26  
27 505 related to the batholith. Garnet websterites (also referred to as high-Mg pyroxenites by Lee et al.,  
28  
29 506 2006) and garnet peridotites have slightly more depleted isotopic values indicative of a  
30  
31 507 subcontinental *enriched* lithospheric mantle (DePaolo, 1981). The similarity in radiogenic isotopes  
32  
33 508 between arclogites and batholith also argues against massive upper crustal contamination during  
34  
35 509 the evolution of the arc, since the pre-batholithic framework of the Sierra Nevada is significantly  
36  
37 510 more enriched in radiogenic isotopes (Ducea, 2001). Whatever assimilation of pre-existing crustal  
38  
39 511 rocks occurred must have taken place in the deepest crustal hot zone.  
40

41 512  
42 513 Oxygen isotopes add important constraints on the amount of local pre-existing crust that has been  
43  
44 514 recycled in these systems. Sierra Nevada whole rock  $\delta^{18}\text{O}$  calculated based on laser ablation  
45  
46 515 individual mineral measurements (clinopyroxenes, garnets, amphiboles) within arclogites are 6.5-  
47  
48 516 8.5‰ relative to SMOW (Standard Mean Ocean Water), with an average of 7.5‰. This is  
49  
50 517 significantly higher than mantle values (typically  $\delta^{18}\text{O}$  of 5.3-5.5 ‰) and those of garnet  
51  
52 518 websterites from the Sierra Nevada ( $\delta^{18}\text{O}$  = 6-6.5 ‰). These values argue strongly for the  
53  
54 519 incorporation of sedimentary rocks that were buried to lower crustal levels after having interacted  
55  
56 520 with the hydrosphere (Ducea, 2002). Metasedimentary xenoliths are known from the central Sierra  
57  
58 521 Nevada (Chin et al., 2013, Ducea and Saleeby 1996, 1998b) and are most likely miogeoclinal  
59  
60 522 (passive margin) rocks transferred to the deep crust through some combination of thrusting from  
61  
62 523 the east (Ducea, 2001, DeCelles et al., 2009) and convective downward flow from above (e.g.,  
63  
64  
65

524 Saleeby, 1990; Paterson and Farris, 2008). Since these sedimentary rocks have  $\delta^{18}\text{O}$  around 10 ‰  
525 on average, one can estimate that about 15-25% of the mass of the arclogite-batholith system is  
526 made of these materials. This constraint is important in that it documents a non-trivial amount of  
527 assimilation of local lower crust, bringing the size of the postulate “root” to no more than twice,  
528 and probably more likely ~1.5 times, the size of the batholith.

## 8. Ages

530  
531  
532 There are two successful methods employed so far in the dating of arclogites: (a) Sm-Nd or Lu-Hf  
533 garnet (and another mineral or whole rock) isochron geochronology or (b) zircon or titanite U-Pb  
534 chronology. Since the community has only recently become aware of the presence of accessory  
535 zircon in arclogites (see Rautela et al. 2020), we expect most future chronology studies of these  
536 rocks will be done by U-Pb. Only two studies so far have attempted to measure U-Pb ages on  
537 titanite, which appears to be reset ages (Chin et al., 2015; Erdman et al., 2016). Garnets are great  
538 candidates for Sm-Nd or Lu-Hf chronology; however, the hot environments in which these rocks  
539 form and possibly reside in for long periods of time renders them susceptible to resetting, as the  
540 closure temperatures for these techniques are in the 600-900 °C range (Ducea and Saleeby, 1998b,  
541 Wendtland et al., 1996). An additional complication comes from textural observations and  
542 chemical zonation patterns suggesting that garnet growth can occur during cooling of the sub-  
543 batholithic root to temperatures as low as ~600 °C (Smith et al., 1994; Rautela et al., 2020). In  
544 these circumstances, garnets are likely to yield ages younger than the corresponding arc (perhaps  
545 10s of Ma younger, if the cooling rate is slow). On the other hand, if isochron ages of arclogites  
546 are much older than their corresponding arc, we must reject the developing hypothesis for the  
547 origin of these rocks. Below, we give examples of ages measured so far in these types of rocks  
548 along with their significance, implications, and limitations.

549  
550 The Sierra Nevada arclogites are cogenetic with the surface batholith. This has been established  
551 not only by the coherence of isotopic measurements between the arclogites and the surface Dinkey  
552 Creek and Shaver Intrusive suites but also by age dating using garnet-clinopyroxene Sm-Nd  
553 chronology (Ducea and Saleeby, 1998b; Chin et al., 2015). The ages of these assemblages are 80-  
554 120 Ma (with relatively large errors typical for garnet Sm-Nd dating in this age range), coincident

1  
2  
3  
4 555 with the age of the surface batholith. The Sierra Nevada arclogites remained in place for at least  
5  
6 556 70 Myr after the cessation of batholith-forming magmatism, since they came up as cold xenoliths  
7  
8 557 entrained in Miocene volcanic rocks that erupted through the batholith. Cooling of these rocks  
9  
10 558 commenced with the demise of the great batholith at 80 Ma and they were never heated regionally  
11  
12 559 again. The coincidence of isotopic characteristics (Ducea, 2002) and Sm-Nd garnet ages (Ducea  
13  
14 560 and Saleeby, 1998b; Chin et al., 2015) between the arclogites and the upper crustal batholith was  
15 561 taken to show these arclogites are sub-batholith rocks.  
16

17 562  
18  
19 563 Mercaderes arclogites have been dated to around  $5\pm 20$  Ma by multi-grain garnet and whole rock  
20  
21 564 Sm-Nd isochron (Ducea, unpublished) and to  $5\pm 5$  Ma by garnet Lu-Hf isochron (Bloch et al.,  
22  
23 565 2017) (same rock samples). Given the extremely large half-lives of these systems, 5 Ma ages come  
24  
25 566 with errors that make these numbers indistinguishable from zero ages. This is not surprising  
26  
27 567 because the temperatures recorded in these rocks exceed  $1000^{\circ}\text{C}$  (and the eruption ages are close  
28  
29 568 to zero) so even if they formed at a distinct age in the past these isochrons would be reset.

30 569  
31  
32 570 Central Arizona arclogites have Sm-Nd garnet ages that are largely reset to a mid-Cenozoic value  
33  
34 571 (Esperanca et al., 1988, Chapman et al., 2020, Figure 7). These rocks have been dated by zircon  
35  
36 572 U-Pb to be Mesozoic. However, because the sub-Arizona lowermost crust was hot and was likely  
37  
38 573 part of a thick and magmatically active orogenic plateau until around the end of the Oligocene (J  
39  
40 574 Chapman et al., 2015), these rocks stayed above the closure temperatures for these systems long  
41  
42 575 after they formed (Rautela et al., 2020). An Eocene (57 Ma) titanite U-Pb age for one arclogite  
43 576 from Chino Valley (Chin et al., 2015) is consistent with these findings.  
44

45 577  
46  
47 578 The discovery of zircon in arclogites (Smith et al., 1994; Chapman et al., 2020, Rautela et al. 2020,  
48  
49 579 Figure 8) paves the way for new geochronologic efforts aimed at unraveling their igneous  
50  
51 580 crystallization ages. Since these rocks were in equilibrium with intermediate magmas, the presence  
52  
53 581 of zircon is not surprising. Rautela et al. (2020) show that the central Arizona arclogites have U-  
54  
55 582 Pb zircon ages coincident with the major pulses of magmatism in the California arc (Figure 8) and  
56  
57 583 therefore argue that these arclogites represent the southern California arc root that was translated  
58  
59 584 eastward toward the continental interior during the Laramide orogeny (Chapman et al., 2020).  
60  
61 585 Future studies of xenoliths or other rocks suspected to be arclogites will certainly use zircon U-Pb  
62  
63  
64  
65

1  
2  
3  
4 586 as a main tool for dating their formation age. The only difficulties in this approach is that sample  
5  
6 587 size is usually small in xenoliths and recovery of zircon is not always straightforward (Rautela et  
7  
8 588 al., 2020).

9 589

## 10 590 **9. Thermobarometry: modern and decayed**

11  
12 591

13  
14  
15 592 Thermometry of arclogitic rocks is performed via classic garnet-clinopyroxene (and  
16  
17 593 orthopyroxene when present; Ellis and Green, 1979 calibration or more modern updates, e.g.  
18  
19 594 Nakamura, 2009), garnet-amphibole calibrations, Ti-in-zircon thermometry (Watson et al., 2006),  
20  
21 595 and garnet-clinopyroxene rare-earth element (REE) thermobarometry (Sun and Liang, 2015).  
22  
23 596 Barometry is performed on orthopyroxene-garnet pairs (using Harley and Green, 1982, Harley,  
24  
25 597 1984 or equivalent Al-in-orthopyroxene in equilibrium with garnet barometers) whenever  
26  
27 598 orthopyroxene (particularly when included in garnets) is present, even in small amounts.  
28  
29 599 Otherwise the garnet-clinopyroxene barometer (Mukhopadhyay, 1989) is used. Another method is  
30  
31 600 to calculate minimum pressures using garnet-pyroxene-plagioclase-quartz barometers (Perkins  
32  
33 601 and Newton, 1981; Newton and Perkins, 1982 or equivalent) (lack of quartz and feldspar providing  
34  
35 602 a minimum estimate). In more recent papers, some arclogite pressures and temperatures were  
36  
37 603 determined using the Gibbs free energy minimization software package THERIAK-DOMINO  
38  
39 604 (deCapitani & Petrakakis, 2010). A good example of this method is a recent study of arclogites  
40  
41 605 from the central Arizona localities (Rautela et al., 2020).

42  
43 606

44  
45 607 Despite the difficulty of estimating pressures on garnet-clinopyroxene rocks, it is fairly well  
46  
47 608 established that arclogites equilibrated between 1.5 GPa and 2.5 GPa at all known localities and  
48  
49 609 that they transition to granulitic assemblages at lower pressures. This is precisely the pressure  
50  
51 610 range over which garnet- and pyroxene-rich residues are predicted by experimental petrology to  
52  
53 611 be stable (e.g. Rapp and Watson, 1995). One published arclogite pressure determination (0.33 GPa  
54  
55 612 at 801 °C, Chin et al., 2015), based on the new garnet-clinopyroxene REE thermobarometer of Sun  
56  
57 613 and Liang (2015), is significantly lower than the 1.5-2.5 GPa range. We consider this value to be  
58  
59 614 spurious given that granulitic assemblages are predicted at those conditions and also because the  
60  
61 615 LREE distribution in clinopyroxene from this sample is significantly lower than that expected at  
62  
63 616 equilibrium (E. Chin, personal communication, 2020).

617

None of the arclogites studied so far display mineral chemistry (and by inference barometric) evidence for major upward or downward vertical movement, with downward migration being relevant to foundering. Some form of foundering has been postulated by Bloch et al. (2017) for the Mercaderes arclogites, but this is more of a proposed hypothesis rather than a valid interpretation due to the fact that evidence for this process does not exist at the mineral grain scale in these arclogites. Garnet websterites and garnet peridotites from Sierra Nevada and Colombian locations, which originate at greater pressures (1.5 to >4 GPa) than arclogites, are not related to foundering and instead represent sub-continental lithospheric mantle assemblages (Mukhopadhyay and Manton, 1994, Ducea and Saleeby, 1996, Lee et al., 2001, Rodrigues Vargas et al., 2005) (Figure 9).

628

All xenolithic arclogites display well constrained temperatures in the range of 700-950 °C (Figure 9). The only outliers are arclogites measured by Bloch et al. (2017), which are much hotter (1150 -1250 °C) than the 700-900 °C temperatures reported for similar assemblages by Weber et al. (2002). It is unclear why this discrepancy exists between the Bloch et al. study and all other temperature measurements of arclogitic assemblages. Garnet websterites and peridotites also record much higher temperatures with estimates similar to those for arclogites reported by Bloch et al. (2017). However, altogether, the temperatures recorded on arclogites in studies from California (Ducea and Saleeby, 1996; Lee et al., 2006; Chin et al., 2015), Arizona (Esperanca et al., 1988, Smith et al., 1994, Erdman et al., 2016, Rautela et al., 2020), the Kohistan arc (Dhuime et al., 2009), and in Beni Bousera (Gysi et al., 2011) are consistent with the relatively limited temperature range known to define the sub-arc lower crust (Depine et al., 2008), which is near-isothermal with a 800-900 °C temperature range.

641

An intriguing aspect of arclogite thermobarometry is the apparent negative PT slope of the Sierra Nevada arclogitic xenoliths, which has been produced independently on at least two datasets using different samples (Mukhopadhyay, 1994, Ducea and Saleeby, 1996). Evidently, prior to convective removal, these rocks had cooled from near-magmatic temperatures to the much colder conditions of the late Cenozoic Sierra Nevada (Ducea and Saleeby, 1996, 1998a). A likely explanation for such cooling is the refrigeration of the Sierra Nevada from below (Dumitru, 1990)

1  
2  
3  
4 648 immediately following the cessation of arc magmatism and during the Laramide orogeny. Another  
5  
6 649 explanation was that the negative slope mimics the solidus of wet basalts (amphibolites) and that  
7  
8 650 temperatures locked in represent near solidus values (Saleeby et al., 2003).  
9

## 10 651 **10. Densities of the hot zones**

11  
12 652  
13 653  
14  
15 654 It is well known that arclogites are denser than the underlying mantle (Ducea, 2002, Lee, 2014,  
16  
17 655 Lee and Anderson, 2015 and references therein) as garnet and other phases are all among the  
18  
19 656 densest rock-forming minerals in an igneous environment. Consequently they will be negatively  
20  
21 657 buoyant with respect to the underlying mantle and will likely founder, although the size of  
22  
23 658 founder fragments, the frequency of foundering events, and the consequences of foundering on  
24  
25 659 magmatism and surface evolution are debated (Kay and Kay, 1993, Ducea and Saleeby, 1998a,  
26  
27 660 Jull and Kelemen, 2001, Lee, 2014). These aspects are summarized in the companion paper (Ducea  
28  
29 661 et al., 2020). Here, we point out that while arcs are active, the negative buoyancy argument may  
30  
31 662 be offset by the presence of positively buoyant granitic partial melt in the deep crustal hot zones  
32  
33 663 (Bowman and Ducea, 2020 in prep.)  
34

35 664  
36  
37 665 Large areas of partial melt are known to exist beneath the frontal arc of the southern and central  
38  
39 666 Andes and beneath the Altiplano-Puna toward the back arc (Ward et al., 2017, Delph et al., 2017,  
40  
41 667 Gonzales Vidal et al., 2018). While researchers originally focused on a mid-crustal (~20 km deep)  
42  
43 668 partial melt reservoir in the Altiplano-Puna (Chiemelowski et al., 1999) named the “Altiplano-  
44  
45 669 Puna Magma Body”, it is now clear that partial melting is extensive in the lowermost part of the  
46  
47 670 central Andean crust in areas where arc magmas are present at the surface. This is not surprising  
48  
49 671 and is predicted by most models of intermediate storage of arc magmas (Hildreth and Moorbaht,  
50  
51 672 1988, Dufek and Bergantz, 2005, Annen et al., 2006 and many others).  
52

53 673  
54  
55 674 If one assumes that the average melt stored in the lowermost crust in an arclogitic reservoir is  
56  
57 675 similar to the major element average of Andean volcanoes or North American batholiths (Ducea  
58  
59 676 et al., 2015), one can calculate the density of the arclogite-intermediate magma system at depth.  
60  
61 677 Densities of liquids are calculated using Bottinga and Weill (1970) and inserted into a modified  
62  
63 678 version of Abers and Hacker (2016) to average the density of the system (Figure 10).  
64  
65

679

Figure 10 shows that for melt fractions of 0.22 (melt percentage of 22%) and higher (which are expected as discussed elsewhere in this review), the “hot zone” will not be negatively buoyant while magma is present even if all cumulates are arclogitic (Bowman and Ducea, 2020). As magma is extracted out of this reservoir (and evidence suggests that it takes place in peaks and lulls, Ducea and Barton, 2007), the density of the root increases significantly (up to 600 kg/m<sup>3</sup>); post-arc cooling of the root contributes additionally to an increase of density (150 kg/m<sup>3</sup>). However, for as long as the melt fraction remains at around 22% or more in an active arc, the root is not negatively buoyant, and this is an important constraint to keep in mind when one models specific dripping scenarios.

## 11. Crustal or mantle rocks?

Arguably, arclogites are petrologically crustal rocks; they represent the processed residues (cumulates or restites) of mafic melts extracted out of the mantle at subduction zones. They are, however, mantle-like rocks because they are ultramafic in composition and have densities and seismic velocities similar to the Earth’s upper mantle (Ducea, 2002, Lee, 2014). Since they are located in the deepest parts of the crust in active arc environments, the question is: are arclogites identified as crustal or sub-crustal rocks by geophysical techniques?

The continental crust to mantle transition, known as the Mohorovicic discontinuity or simply the Moho, is typically well-defined in areas that are either cratonic or have undergone extensional collapse at the end of orogenic cycles (Meissner, 1986). The Basin and Range in the Western US is one such example (Klemperer et al., 1986), where the Moho is fairly flat and typically found at 30 km below the surface. The Sierra Nevada batholith, which presumably has undergone foundering and has been affected by nearby extension, has a flat and well-defined Moho at 33 km (Fliedner and Ruppert, 1996; Wernicke et al., 1996). Beneath active convergent margins and especially those that contain magmatic arcs, it is much more difficult to resolve depth to Moho using seismic data. For example, the depth to Moho in the Puna plateau in South America ranges from 35 km to over 70 km within 1-degree grids over which teleseismic receiver function data was acquired (Yuan et al., 2002), although better resolutions have been more recently obtained

1  
2  
3  
4 710 (Assumpcao et al., 2013, Gonzales Vidal et al., 2018). Additionally, large discrepancies exist  
5  
6 711 between the seismically determined Moho and the Moho inferred from Bouguer anomalies under  
7  
8 712 the Andean frontal arc (Tassara et al., 2007). These discrepancies bring to light the question of  
9  
10 713 whether the seismically defined Moho in these areas truly represents the “petrologic” transition  
11  
12 714 from crustal mafic to mantle ultramafic (peridotitic) lithologies as implied by most studies seeking  
13  
14 715 the location of the Moho, or whether the seismic and petrologic “Mohos” are actually rather  
15  
16 716 different in sub-arc environments (Herzberg et al., 1983, Griffin and O’Reilly, 1987). It is quite  
17  
18 717 plausible that the transition from granulite to arclogite facies in deep crustal hot zones is recorded  
19  
20 718 as the seismic Moho in these areas, which in reality may be over 20-30 km shallower than the  
21  
22 719 transition to true lithospheric mantle (Figure 1). The complexities that arise from the addition of  
23  
24 720 partial melt (discussed in Section 10) additionally influence the depth to Moho; a greater fraction  
25  
26 721 of melt within hot zones would drive both the density of the residue and the location of the Moho  
27  
28 722 towards greater depths. Consequently, it may be impossible to identify a single major refractor that  
29  
30 723 represents the Moho beneath thick arcs like the modern Andes, and in particular the central Andes  
31  
32 724 and parts of the northern Andes. At peak magmatism and before melt has been largely extracted  
33  
34 725 from hot zones, the seismic and petrologic Moho may coincide and are deep, whereas at the end  
35  
36 726 of magmatism but before any major foundering, the seismic Moho may be tens of km shallower  
37  
38 727 than the petrologic one (Figure 1). The post-foundering Moho may be a much sharper feature  
39  
40 728 (Jagoutz and Behn, 2013).  
41  
42 729

## 41 730 **12. Continental evolution implications**

42 731  
43  
44 732 If the complements to thicker arcs (transitional, thicker island and continental) are mostly  
45  
46 733 arclogites, then their crust-mantle architecture is somewhat unusual in that a dense root of sizable  
47  
48 734 mass develops, perhaps making as much as twice the mass of intermediate magmatic rocks in the  
49  
50 735 upper to middle crust (Figure 1). This picture emerges from many studies of arc sequences in the  
51  
52 736 geologic record (Ducea, 2002, Saleeby et al., 2003, Lee et al., 2006, Jagoutz and Schmidt, 2013).  
53  
54 737 Elevated Sr/Y and La/Yb ratios (Profeta et al., 2015), a lack of Eu anomalies, and other average  
55  
56 738 chemical parameters in surface intermediate volcanics (Mamani et al., 2010) or the corresponding  
57  
58 739 batholith (Ducea et al., 2015) require that many arcs have a deep counterpart, with plagioclase  
59  
60 740 playing only a limited role in magmatic diversification. However, not all arcs display these  
61  
62  
63  
64  
65



1  
2  
3  
4 741 signatures: numerous arcs, including some that are locally exposed to deep crustal levels, are thin  
5  
6 742 enough such that they require only a granulitic residue, not an arclogitic one. For example, both  
7  
8 743 Famatinian (Otamendi et al., 2009) and Salinian (Chapman et al., 2014) arcs lack garnet signatures.  
9  
10 744 Similarly, there is no garnet-rich lower crust where the Sierra Valle Fertil (Otamendi et al., 2009,  
11  
12 745 2012, Walker et al., 2015) or Salinia (Ducea et al., 2003) are exposed to 30 km paleodepths.

13 746  
14  
15 747 However, garnet and amphibole (Davidson et al., 2007, Profeta et al., 2015, Ducea et al., 2015)  
16  
17 748 signatures resembling arclogitic residues seem to be dominant in global databases. Simply put, if  
18  
19 749 only Sr/Y and the REEs are taken into consideration, the average of most young Cordilleran  
20  
21 750 batholiths are intermediate rocks straddling the border between adakitic and non-adakitic  
22  
23 751 compositions (Ducea et al., 2015). In contrast to the original hypothesis for the origin of adakites,  
24  
25 752 the isotopes in all Cordilleran batholiths are inconsistent with slab melting as a main mechanism  
26  
27 753 of magma generation (Ducea and Barton, 2007). Therefore, these garnet and amphibole markers  
28  
29 754 and the lack of a plagioclase signature must have been acquired in a deep crustal, arclogitic-like  
30  
31 755 environment.

32 756  
33  
34 757 Balica et al. (2020) used zircon petrochronology on Hadean to Phanerozoic detrital zircons in an  
35  
36 758 effort to calculate the trace elemental chemistry and in particular the REE chemistry of granitoids  
37  
38 759 in equilibrium with those zircons. This global approach showed two remarkably consistent trends  
39  
40 760 over time. First, most of the zircon archive is made of igneous zircons (low U/Th zircons) that  
41  
42 761 crystallized in the Ti-in-zircon temperature window most consistent with granitic melts (650-858  
43  
44 762 °C). Second, granitoids of all ages require a garnet-pyroxene-amphibole residue based on the  
45  
46 763 La/Yb and Sm/Yb ratios calculated for whole rocks in equilibrium with these zircons over time  
47  
48 764 (Figure 112). This does not require that the processes taking place at modern convergent margins  
49  
50 765 have operated since the Hadean; granitoids and by inference the continental crust could have been  
51  
52 766 extracted out of thick oceanic-like plateaus or other tectonic environments (Dhuime et al., 2015).  
53  
54 767 However, the global zircon dataset does imply that conditions for arclogite generation must have  
55  
56 768 existed since the time in Earth's history when felsic magmas began being generated.

57 769  
58  
59 770 Yet a still common perception is that only continental (also known as Andean or Cordilleran) arcs  
60  
61 771 can be complemented by arclogites. This raises the following question: if Andean/Cordilleran arcs

1  
2  
3  
4 772 are continental crust-forming factories, how can continental crust only be formed on pre-existing  
5  
6 773 continental crust, and how did it all start? The resolution is two-fold: first, the widely held opinion  
7  
8 774 that island arcs are mafic (Rudnick, 1995) has no real global basis in the modern geologic record  
9  
10 775 and has been repeatedly proven false as some modern island arcs are intermediate in bulk  
11  
12 776 chemistry (e.g. Gill, 1981, Jagoutz and Kelemen, 2015). Different arcs built onto oceanic or  
13  
14 777 continental crust can in reality have surprisingly variable average silica contents – some  
15  
16 778 continental arcs are more mafic on average than other oceanic ones (Ducea et al., 2015). Secondly,  
17  
18 779 it has also been suggested that some island arcs of the recent geologic past have been thickened to  
19  
20 780 more than 40 km (Jagoutz and Schmidt, 2012, Davidson and Arculus, 2006). Environments that  
21  
22 781 are more easily studied on land (the western North American batholiths or the central Andes  
23  
24 782 volcanic arcs) do exist in an intra-oceanic realm as well.  
25

26 783  
27 784 Overall, the arclogite model proposes that these rocks complement large intermediate magmatic  
28  
29 785 arcs at depth. Arclogite formation drives silica up in the corresponding melt due to the  
30  
31 786 crystallization of the low silica minerals that characterize these assemblages. Melt extraction from  
32  
33 787 lower crustal melt-solid zones allows these arclogites to reach a critical density such that they  
34  
35 788 founder into the mantle and leave behind a continental crust that is intermediate in composition  
36  
37 789 (Ducea, 2002, Lee, 2014, Lee and Anderson 2015).  
38

### 39 791 **13. Implications moving forward**

40  
41 792  
42  
43 793 The big picture implications and questions for the arclogite model are:  
44

45 794  
46 795 (1) With clinopyroxene, garnet, amphibole, and Fe-Ti oxides within the residue, intermediate rocks  
47  
48 796 formed at magmatic arcs have a much easier path to high silica contents than magmatic systems  
49  
50 797 that start out with bulk basaltic chemistries and form granulitic residues. Garnet, amphibole, and  
51  
52 798 all oxides have lower silica (or no silica in the case of oxides) than a basalt. Plagioclase, in contrast,  
53  
54 799 has a silica content that is similar to or higher than a basaltic bulk composition, while  
55  
56 800 clinopyroxene is neutral in that respect;

57 801  
58  
59  
60  
61  
62  
63  
64  
65

1  
2  
3  
4  
5  
6  
7  
8  
9  
10  
11  
12  
13  
14  
15  
16  
17  
18  
19  
20  
21  
22  
23  
24  
25  
26  
27  
28  
29  
30  
31  
32  
33  
34  
35  
36  
37  
38  
39  
40  
41  
42  
43  
44  
45  
46  
47  
48  
49  
50  
51  
52  
53  
54  
55  
56  
57  
58  
59  
60  
61  
62  
63  
64  
65

802 (2) After significant melt extraction, the extreme density of these materials make the roots of arcs  
803 prone to detachment, removal (foundering), and integration into the convective mantle. These  
804 rocks are significantly denser than typical oceanic eclogite in subduction systems because they are  
805 richer in garnet, are more Fe-rich, and contain other dense phases, like magnetite and ilmenite, that  
806 contribute significantly to the negative buoyancy;

807  
808 (3) After removal via some form of foundering into the mantle, these assemblages are prone to  
809 remelting (Elkins Tanton 2007, Ducea et al., 2013, Tang et al., 2019). It is critical to understand  
810 the products of this process, as these types of garnet pyroxenites are already massively depleted of  
811 a felsic component. Arclogitic garnet pyroxenites thus significantly differ from generic basaltic  
812 garnet pyroxenites (Hirschmann and Stolper, 1996, Peterman and Hirschmann, 2003), which are  
813 capable of producing intermediate melts or at least a sizable fraction of mafic melt compared to  
814 peridotite.

815  
816 (4) If these assemblages undergo long term storage in the mantle, what is the isotopic signature of  
817 a long-term archived arclogite if its signature were to reappear in an oceanic island basalt (Tatsumi,  
818 2000, Tatsumi, 2005)? Where in the mantle geodynamics isotopic space (Zindler and Hart, 1986)  
819 can one identify ancient recycled arclogites?

820  
821 These issues and questions are dealt with in a companion paper (Ducea et al., 2020).

822  
823 Acknowledgments. MND: I acknowledge support from US National Science Foundation grant  
824 EAR 1725002 and the Romanian Executive Agency for Higher Education, Research, Development  
825 and Innovation Funding project PN-III-P4-ID-PCCF-2016-0014. I want to thank my students and  
826 postdocs Steven Kidder, Peter Luffi, Alan Chapman, Jay Chapman, Antoine Tryantafyllou,  
827 Robinson Cecil, Costi Balica, and Emilie Bowman for their contributions to arclogite science  
828 (direct or indirect), which are reflected in this paper. I thank my PhD adviser Jason Saleeby and  
829 my committee members Peter Wyllie, Hugh Taylor Jr and Ed Stolper for guiding me in my early  
830 studies. I am forever indebted for the gracious reviews I received from Calvin Miller and Robert  
831 Kay on my early manuscripts: they were not just constructive they were career defining. I have  
832 learned a lot on the subject of this paper from some extraordinary peers that I am lucky to have

within reach of an email or in the building: Cin-Ty Lee, Peter DeCelles, Claire Currie, George Bergantz, and George Zandt. ADC: I would like to thank my PhD advisor Jason Saleeby (yes, MND and I share the same academic parentage), who brought arclogites to my attention, and my coauthor for alerting me to the existence and significance of central Arizona arclogite xenolith localities. Support from NSF grant EAR-1524768 allowed myself and my amazing students Ojashvi Rautela, Jessie Shields, and Michael Murphy to study central Arizona arclogite nodules in more detail, for which I am grateful. This effort benefitted from field and laboratory assistance by D. Abboud, B. Hunter, and J. Thole and discussions with E. Chin, S. Esperança, C.-T. Lee, D. Smith.

**References**

Abers, G., Hacker, B., 2016. A MATLAB toolbox and Excel workbook for calculating the densities, seismic wave speeds, and major element compositions of minerals and rocks at pressure and temperature. *Geochemistry Geophysics Geosystems*, 17, 616–624.

Anderson, D.L., 2005, Large igneous provinces, delamination, and fertile mantle: *Elements*, v. 1, p. 271–275, <https://doi.org/10.2113/gselements.1.5.271>.

Annen C, Blundy JD, Sparks RSJ. 2006. The genesis of intermediate and silicic magmas in deep crustal hot zones. *Journal of Petrology* 47:505-39.

Anczkiewicz, R. and Vance, D., 2000, Isotopic constraints on the evolution of metamorphic conditions in the Jijal Patan Complex and Kamila Belt of the Kohistan Arc, Pakistan Himalaya. In: Khan, M. A., Treloar, P. J., Searle, M. P. & Jan, M. Q. (eds) *Tectonics of the Nanga Parbat Syntaxis and the Western Himalaya*. Geological Society, London, Special Publications 170, 321-331.

Arculus, R.J., and Smith, D., 1979, Eclogite, pyroxenite, and amphibolite inclusions in the Sullivan Buttes latite, Chino Valley, Yavapai County, Arizona, *The Mantle Sample: Inclusions in Kimberlites and other Volcanics*, American Geophysical Union, Washington, DC, p. 309-317.

Arndt NT, Goldstein SL. 1989. An open boundary between lower continental crust and mantle: its role in crust formation and crustal recycling. *Tectonophysics* 161:201–12.

Assumpcao, M., Feng, M., Tassara, A., Julia, J. 2013, Models of crustal thickness for South America from seismic refraction, receiver functions, and surface wave tomography, *Tectonophysics*, 609, 82-96.

- 1  
2  
3  
4 872 Aulbach, S., Arndt, N., 2019. Eclogites as palaeodynamic archives: evidence for warm (not hot)  
5 873 and depleted (but heterogeneous) Archaean ambient mantle. *Earth and Planetary Science Letters*,  
6 874 505, 162–172.  
7  
8 875  
9 876 Balica, C., M.N. Ducea, G.E. Gehrels, J. Kirk, R.D. Roban, P. Luffi, J.B. Chapman, A. Triantafyllou,  
10 877 J. Guo, A.M. Stoica, J. Ruiz, I. Balintoni, L. Profeta, D. Hoffman, L. Petrescu, 2020, A zircon  
11 878 petrochronologic view on granitoids and continental evolution, *Earth and Planetary Science*  
12 879 *Letters*, 531, paper 11605 <https://doi.org/10.1016/j.epsl.2019.116005>.  
13  
14 880  
15 881 Banno, S., 1970. Classification of eclogites in terms of physical conditions of their origin. *Physics*  
16 882 *of the Earth and Planetary Interiors*, 3, 405–421.  
17  
18 883  
19 884 Basaltic Volcanism Study Project, *Basaltic Volcanism in the Terrestrial Planets*, Pergamon, New  
20 885 York, 1981.  
21 886  
22 887 Bloch, E., Ibanez-Mehia, M., Murray, K., Vervoort, J., Muntener, O., 2017, Recent crustal  
23 888 foundering in the Northern Volcanic Zone of the Andean arc: Petrological insights from the roots  
24 889 of a modern subduction zone, *Earth and Planetary Science Letters*, 476, 47-58.  
25  
26 890  
27 891 Bottinga, Y., Weill, D.F., 1970 Densities of liquid silicate systems calculated from partial molar  
28 892 volumes of oxide components, *Am J Sci*, 269:169-182.  
29  
30 893  
31 894 Burg, J.-P., Bodinier, J.-L., Chaudhry, S., Hussain, S. & Dawood, H. ,1998, Infra-arc mantle-crust  
32 895 transition and intra-arc mantle diapirs in the Kohistan Complex (Pakistani Himalaya): petro-  
33 896 structural evidence. *Terra Nova* 10, 74-80.  
34  
35 897  
36 898 Carroll, M.R., Wyllie, P.J., 1990, The system tonalite-H<sub>2</sub>O at 15 kbar and the genesis of calc-  
37 899 alkaline magmas: *American Mineralogist*; 75 (3-4): 345–357  
38  
39 900  
40 901 Chapman, A.D., Riggs, N., Ducea, M.N., Saleeby, J.B., Rautela, O., and Shields, J., 2019, Tectonic  
41 902 development of the Colorado Plateau Transition Zone, central Arizona: Insights from lower  
42 903 lithosphere xenoliths and volcanic host rocks, in Pearthree, P.A., ed., *Geologic Excursions in*  
43 904 *Southwestern North America: Geological Society of America Field Guide* 55, p. 209–235,  
44 905 [https://doi.org/10.1130/2019.0055\(09\)](https://doi.org/10.1130/2019.0055(09)).  
45  
46 906  
47 907 Chapman, A. D., Ducea, M. N., Kidder, S., and Petrescu, L., 2014, Geochemical constraints on  
48 908 the petrogenesis of the Salinian arc, central California: Implications for the origin of intermediate  
49 909 magmas: *Lithos*, v. 200, p. 126-141.  
50  
51 910  
52 911 Chapman, A. D., Rautela, O., Shields, J. E., Ducea, M. N., & Saleeby, J. B., 2020, Fate of  
53 912 Continental Lower Crust and Upper Mantle During Shallow-Angle Subduction: the Laramide  
54 913 Example. *GSA Today*, v. 30, <https://doi.org/10.1130/GSATG412A.1>.  
55  
56 914  
57 915 Chapman, A.D., Ducea, M.N., McQuarrie, N., Coble, M., Petrescu, L., Hoffman, D., 2015.  
58 916 Constraints on plateau architecture and assembly from deep crustal xenoliths, northern Altiplano  
59 917 (SE Peru). *Geological Society of America Bulletin* 127, 1777-1797.  
60  
61  
62  
63  
64  
65

- 1  
2  
3  
4 918  
5 919 Chapman, J.B., Ducea, M.N., DeCelles, P.G., Profeta, L., 2015. Tracking changes in crustal  
6 920 thickness during orogenic evolution with Sr/Y: An example from the North American Cordillera.  
7 921 *Geology* 43, 919-922.  
8 922  
9  
10 923 Chin, E., Lee, C.T., Luffi, P., 2012, Deep lithospheric thickening and refertilization beneath  
11 924 continental arcs: case study of the P, T and compositional evolution of peridotite xenoliths from  
12 925 the Sierra Nevada, California, *Journal of Petrology*, v. 53, p. 477-511.  
13 926  
14 927 Chin, E.J., Lee, C.-T.A., Tollstrup, D.L., Xie, L., Wimpenny, J. B., Yin, Q. Z., 2013, On the origin  
15 928 of hot metasedimentary quartzites in the lower crust of continental arcs, *Earth Planet. Sci. Lett.*,  
16 929 361, 120–133.  
17 930  
18 931 Chin, E.J., Lee, C.-T.A., Barnes, J.D., 2014. Thickening, refertilization, and the deep lithospheric  
19 932 filter in continental arcs: constraints from major and trace elements and oxygen isotopes. *Earth*  
20 933 *Planet. Sci. Lett.* 397, 184–200.  
21 934  
22 935 Chin, E.J., Lee, C.T.A. and Blichert-Toft, J., 2015. Growth of upper plate lithosphere controls  
23 936 tempo of arc magmatism: Constraints from Al-diffusion kinetics and coupled Lu-Hf and Sm-Nd  
24 937 chronology. *Geochemical Perspectives Letters*, 1, pp.20-32.  
25 938  
26 939 Chmielowski, J., Zandt, G., and Haberland, C., 1999, The central Andean Altiplano-Puna magma  
27 940 body, *Geophysical Research Letters*, 26, 783-786.  
28 941  
29 942 Coleman, R.G., Lee, D.E., Beatty, L.B., Brannock, W.W., 1965. Eclogites and eclogites: their  
30 943 differences and similarities. *Geological Society of America Bulletin* 76, 483–508.  
31 944  
32 945 Conrad, W.K., Kay R.W., 1984, Ultramafic and Mafic Inclusions from Adak Island:  
33 946 Crystallization History, and Implications for the Nature of Primary Magmas and Crustal Evolution  
34 947 in the Aleutian Arc, *Journal of Petrology*, 25, 88–125.  
35 948  
36 949 Currie, C., Ducea, M.N., and DeCelles, P.G., Geodynamic models of Cordilleran orogens:  
37 950 Gravitational instability of magmatic arc roots, in DeCelles, P.G., Ducea, M.N., Carrapa B., and  
38 951 Kapp, P. (editors), “Geodynamics of a Cordilleran Orogenic System: The Central Andes of  
39 952 Argentina and Northern Chile”, *Geological Society of America Memoir*, 212, p. 1-22; 2015.  
40 953  
41 954 Davidson J, Turner S, Handley H, Macpherson C, Dosseto A. 2007. Amphibole "sponge" in arc  
42 955 crust? *Geology* 35:787-90  
43 956  
44 957 Davidson JP, Arculus RJ. 2006. The significance of Phanerozoic arc magmatism in generating  
45 958 continental crust. In *Evolution and Differentiation of the Continental Crust*, ed. M Brown, T  
46 959 Rushmer, pp. 135-72. Cambridge: Cambridge University Press  
47 960  
48 961 DeBari SM, Kay SM, Kay RW. 1987. Ultramafic xenoliths from Adagdak volcano, Adak, Aleutian  
49 962 islands, Alaska: deformed igneous cumulates from the Moho of an island arc. *J. Geol.* 95:329–41  
50 963  
51  
52  
53  
54  
55  
56  
57  
58  
59  
60  
61  
62  
63  
64  
65

1  
2  
3  
4 964 de Capitani, C. & Petrakakis, K., 2010, The computation of equilibrium assemblage diagrams with  
5 965 Theriak/ Domino software, *American Mineralogist*, 95, 1006-1016.  
6 966  
7 967 DeCelles, P., Ducea, M.N., Kapp, P., Zandt, G., 2009. Cyclicality in Cordilleran orogenic systems.  
8 968 *Nat. Geosci.* 2, 251–257.  
9 969  
10 970 Delph, J.R., Ward, K.M., Zandt, G., Ducea, M.N., Beck, S.L., 2017. Imaging a magma plumbing  
11 971 system from MASH zone to magma reservoir. *Earth and Planetary Science Letters* 457, 313-324.  
12 972  
13 973 DePaolo, D.J., 1981, A Neodymium and strontium study of the Mesozoic calc-alkaline granitic  
14 974 batholiths of the Sierra Nevada and Peninsular Ranges, *J. Geophys. Res.*, v. 86, p. 10470-10488.  
15 975  
16 976 Depine GV, Andronicos CL, Phipps-Morgan J. 2008. Near-isothermal conditions in the middle  
17 977 and lower crust induced by melt migration. *Nature* 452:80-3.  
18 978  
19 979 Dhuime B, Bosch D, Garrido CJ, Bodinier JL, Bruguier O, et al. 2009. Geochemical architecture  
20 980 of the lower- to middle-crustal section of a paleo-island arc (Kohistan complex, Jijal-Kamila area,  
21 981 northern Pakistan): implications for the evolution of an oceanic subduction zone. *J. Petrol.* 50:531–  
22 982 69  
23 983  
24 984 Dhuime, B., Wuestefeld, A., Hawkesworth, C.J., 2015. Emergence of modern continental crust  
25 985 about 3 billion years ago. *Nat. Geosci.* 8, 552–554.  
26 986  
27 987 Dodge F.C.W., Calk L.C., and Kistler R.W., 1986, Lower crustal xenoliths, Chinese Peak lava  
28 988 flow, Central Sierra Nevada, *J. Petrol.*, 27: 1277-1304.  
29 989  
30 990 Dodge F.C.W., Lockwood J.P., and Calk L.C., 1988, Fragments of the mantle and crust beneath  
31 991 the Sierra Nevada batholith: Xenoliths in a volcanic pipe near Big Creek, California, *Geol. Soc.*  
32 992 *Am. Bull.*, 100: 938-947.  
33 993  
34 994 Domenick M.A., Kistler R.W., Dodge F.C.W., and Tatsumoto M., 1983, Nd and Sr study of crustal  
35 995 and mantle inclusions from the Sierra Nevada and implications for batholith petrogenesis, *Geol.*  
36 996 *Soc. Am. Bull.*, 94: 713-719.  
37 997  
38 998 Ducea, M., and Saleeby, J., 1996, Buoyancy sources for a large, unrooted mountain range, the  
39 999 Sierra Nevada; Evidence from xenolith thermobarometry, *J. Geophys. Res.*, v. 101, p. 8029-8044.  
40 1000  
41 1001 Ducea, M., Saleeby, J., 1998a, A case for delamination of the deep batholithic crust beneath the  
42 1002 Sierra Nevada, California. *International Geology Review* 40, 78-93.  
43 1003  
44 1004 Ducea, M.N., and Saleeby, J. B., 1998b, The age and origin of a thick mafic-ultramafic keel from  
45 1005 beneath the Sierra Nevada batholith, *Contrib. Mineral. Petrol.*, 133, 169-185.  
46 1006  
47 1007 Ducea, M. N., 2001, The California Arc: thick granitic batholiths, eclogitic residues, lithospheric-  
48 1008 scale thrusting, and magmatic flare-ups, *GSA Today*, v. 11, p. 4-10.  
49 1009  
50  
51  
52  
53  
54  
55  
56  
57  
58  
59  
60  
61  
62  
63  
64  
65

- 1  
2  
3  
41010 Ducea, M.N., 2002. Constraints on the bulk composition and root foundering rates of continental  
51011 arcs: A California arc perspective. *Journal of Geophysical Research: Solid Earth* 107,  
61012 doi:10.1029/2001JB000643.  
81013
- 91014 Ducea, M.N., Kidder, S., Zandt, G., 2003. Arc composition at mid- crustal depths: Insights from  
101015 the Coast Ridge Belt, Santa Lucia Mountains, California. *Geophysical Research Letters* 30,  
111016 doi:10.1029/2002GL016297.  
131017
- 141018 Ducea, M.N., Barton, M.D., 2007. Igniting flare-up events in Cordilleran arcs. *Geology* 35, 1047-  
151019 1050.  
161020
- 171021 Ducea, M.N., Saleeby, J.B., Bergantz, G., 2015. The architecture, chemistry, and evolution of  
181022 continental magmatic arcs. *Annual Review of Earth and Planetary Sciences* 43, 299-331.  
201023
- 211024 Ducea, M.N., Seclaman, A.C., Murray, K.E., Jianu, D., Schoenbohm, L.M., 2013. Mantle-drip  
221025 magmatism beneath the Altiplano-Puna plateau, central Andes. *Geology* 41, 915-918.  
241026
- 251027 Ducea, M. N., & Chapman, A. D. (2018). Sub-magmatic arc underplating by trench and forearc  
261028 materials in shallow subduction systems; A geologic perspective and implications. *Earth-Science*  
271029 *Reviews*, 185, 763–779. doi:10.1016/j.earscirev.2018.08.001  
281030
- 291031 Ducea, M.N., Bowman, E., Chapman, A.D., Balica, C., 2020, Arclogites and their role in  
301032 continental evolution; Part 2: Relationship to batholiths and volcanoes, density and foundering,  
311033 remelting and long-term storage in the mantle, companion paper submitted to this one.  
321034
- 331035 Dufek J, Bergantz GW. 2005. Lower crustal magma genesis and preservation: A stochastic  
341036 framework for the evaluation of basalt-crust interaction. *Journal of Petrology* 46:2167-95.  
371037
- 381038 Dumitru, T. A., 1990, Subnormal Cenozoic geothermal gradients in the extinct Sierra Nevada  
391039 magmatic arc: Consequences of Laramide and post-Laramide shallow angle subduction, *J.*  
401040 *Geophys. Res.*, 95, 4925-4941.  
421041
- 431042 El Atrassi, F., Brunet, F., Chazot, G., Bouybaouène, M., Chopin, C., 2013, Metamorphic and  
441043 magmatic overprint of garnet pyroxenites from the Beni Bousera massif (northern Morocco):  
451044 Petrography, mineral chemistry and thermobarometry, *Lithos*, 179, 231-248.  
471045
- 481046 Ellis, D. J., and E. H. Green, 1979, An experimental study of the effect of Ca upon garnet-  
491047 clinopyroxene Fe-Mg exchange equilibria, *Contrib. Mineral. Petrol.*, 66, 13-22.  
501048
- 511049 Elkins-Tanton, L.T., 2007, Continental magmatism, volatile recycling, and a heterogeneous  
521050 mantle caused by lithospheric gravitational instabilities: *Journal of Geophysical Research*, v. 112,  
531051 B03405, doi:10.1029/2005JB004072.  
541052
- 551053 Erdman, M.E., Lee, C.-T.A., Levander, A., Jiang, H., 2016. Role of arc magmatism and lower  
561054 crustal foundering in controlling elevation history of the Nevadaplano and Colorado Plateau: a  
59  
60  
61  
62  
63  
64  
65



1  
2  
3  
4 1055 case study of pyroxenitic lower crust from central Arizona, USA. *Earth and Planetary Science*  
5 1056 *Letters* 439, 48-57.  
6  
7 1057  
8 1058 Ernst, W.G., 2009, Archean plate tectonics, rise of Proterozoic supercontinentality and onset of  
9 1059 regional, episodic stagnant-lid behavior, *Gondwana Research*, 15, 243-253.  
10 1060  
11 1061 Eskola, P., 1920. The mineral facies of rocks. *Norsk Geologisk Tidsskrift* VI, 143–194.  
12  
13 1062  
14 1063 Esperanca, S., Carlson, R.W., and Shirey, S.B., 1988, Lower crustal evolution under central  
15 1064 Arizona: Sr, Nd, and Pb isotopic and geochemical evidence from mafic xenoliths of Camp Creek,  
16 1065 *Earth and Planetary Science Letters*, v. 90, p. 26-40.  
17  
18 1066  
19 1067 Esperanca, S., Carlson, R.W., Shirey, S.B., and Smith, D., 1997, Dating crust-mantle separation:  
20 1068 Re-Os isotopic study of mafic xenoliths from central Arizona, *Geology*, v. 25, p. 651-654.  
21 1069  
22 1070 Farmer, G.L., Glazner, A.F., and Manley, C.R., 2002, Did lithospheric delamination trigger late  
23 1071 Cenozoic potassic volcanism in the southern Sierra Nevada, California? *Geological Society of*  
24 1072 *America Bulletin*, v. 114, p. 754–768.  
25  
26 1073  
27 1074 Flidner M. and Ruppert S., 1996, 3-dimensional crustal structure of the Southern Sierra Nevada  
28 1075 from seismic fan profiles and gravity modelling, *Geology*, 24: 367-370.  
29  
30 1076  
31 1077 Gao, S., Rudnick, R., Yuan, H.-L., Liu, X.-M., Liu, Y.-S., Xu, W.-L., Ayers, J., Wang, X.-C.,  
32 1078 Wang, Q.-H., 2004. Recycling lower continental crust in the North China craton. *Nature* 432, 892–  
33 1079 897.  
34  
35 1080  
36 1081 Garrido, C. J., Bodinier, J.-L., Burg, J.-P., Zeilinger, G., Hussain, S., Dawood, H., Chaudhry, M.  
37 1082 N. & Gervilla, F. , 2006, Petrogenesis of mafic garnet granulite in the lower crust of the Kohistan  
38 1083 Paleo- arc Complex (Northern Pakistan): Implications for intra-crustal differentiation of island  
39 1084 arcs and generation of continental crust. *Journal of Petrology* 47, 1873-1914.  
40  
41 1085  
42 1086 Ghiorso, M.S., and Sack, R. O., 1995, Chemical Mass Transfer in Magmatic Processes. IV. A  
43 1087 Revised and Internally Consistent Thermodynamic Model for the Interpolation and Extrapolation  
44 1088 of Liquid-Solid Equilibria in Magmatic Systems at Elevated Temperatures and Pressures.  
45 1089 *Contributions to Mineralogy and Petrology*, 119, 197-212  
46  
47 1090  
48 1091 Gill J. 1981. *Orogenic andesites and plate tectonics*. Springer-Verlag, Berlin.  
49 1092  
50 1093 Godard, G., 2001, Eclogites and their geodynamic interpretation: A history, *Journal of*  
51 1094 *geodynamics*, 32, 163-203.  
52  
53 1095  
54 1096 Gonzales Vidal, D., Obermann, A., Tassara, A., Bataille, K., Lupi, M., 2018, Crustal model of the  
55 1097 Southern Central Andes derived from ambient Rayleigh wave tomography, *Tectonophysics*, 744,  
56 1098 215-226.  
57  
58 1099  
59 1100 Green D.H., Ringwood A.E., 1967a, The genesis of basaltic magmas, *Contr Mineral Petrol*  
60  
61  
62  
63  
64  
65

- 1  
2  
3  
41101 15:103–190.  
51102  
61103 Green, D.H., Ringwood, A.E., 1967b. An experimental investigation of the gabbro to eclogite  
81104 transformation and its petrological applications. *Geochimica and Cosmochimica Acta* 31, 767–  
91105 833.  
101106  
111107 Griffin, W. L., and S. Y. O'Reilly, 1986, The lower crust in eastern Australia: Xenolith evidence,  
121108 in *The Nature of the Lower Continental Crust*, edited by J. B. Dawson, et al., *Spec. Publ. Geol.*  
141109 *Soc. Am.*, 24, 363-374.  
151110  
161111 Griffin, W. L., & O'Reilly, S. Y., 1987, Is the continental Moho the crust- mantle boundary?  
171112 *Geology*, 15, 241-244.  
181113  
191114 Gysi, A.P., Jagoutz, O., Schmidt, M.W., Targuisti, K., 2011, Petrogenesis of pyroxenites and melt  
211115 infiltrations in the ultramafic complex of Beni Bousera, northern Morocco. *Journal of Petrology*,  
221116 22, 1679-1735.  
231117  
241118 Harley, S. L., 1984, An experimental study of the partitioning of Fe and Mg between garnet and  
261119 orthopyroxene, *Contrib. Mineral. Petrol.*, 86, 359-373.  
271120  
281121 Harley, S. L., and D. H. Green, 1982, Garnet-orthopyroxene barometry for granulites and  
301122 peridotites, *Nature*, 300, 697-701.  
311123  
321124 Haüy, R.J., 1822. *Traité de minéralogie*. Seconde édition, revue, corrigée et considé-  
331125 rablement augmentée par l'auteur. Bachelier et Huzard, Paris, 4 Vols+atlas (t. II, p. 456; t. IV,  
341126 p. 548).  
351127  
361128 Herzberg, C.T., Fyfe, W.S., and Carr, M.J., 1983, Density constraints on the formation of the  
381129 continental Moho and crust: *Contributions to Mineralogy and Petrology*, v. 84, p. 1–5, doi:  
391130 10.1007/BF01132324  
401131  
411132 Hildreth W, Moorbath S. 1988. Crustal contributions to arc magmatism in the Andes of central  
431133 Chile. *Contributions to Mineralogy and Petrology* 98:455-89.  
441134  
451135 Hirschmann, M.M., and Stolper, E.M., 1996, A possible role for garnet pyroxenite in the origin of  
471136 the “garnet signature” in MORB: *Contributions to Mineralogy and Petrology*, v. 124, p. 185–208,  
481137 doi:10.1007/s004100050184  
491138  
501139 Holland, T.H., 1896. On the origin and growth of garnets and of their micropegmatitic intergrowths  
511140 in pyroxenic rocks. *Records of the geological Survey of India* 29, 20–30+1 pl.  
521141  
531142 Jacob, D.E., 2004. Nature and origin of eclogite xenoliths from kimberlites. *Lithos* 77, 195–316.  
541143  
551144 Jagoutz, O.E., Schmidt, M.W., 2012. The formation and bulk composition of modern juvenile  
561145 continental crust: the Kohistan arc. *Chem. Geol.* 298–299, 79–96.  
571146  
581146  
591146  
60  
61  
62  
63  
64  
65

- 1  
2  
3  
4 1147 Jagoutz O, Behn MD. 2013. Foundering of lower arc crust as an explanation for the origin of the  
5 1148 continental Moho. *Nature* 504:131–34  
6 1149  
7 1149  
8 1150 Jagoutz O, Schmidt MW. 2013. The composition of the foundered complement to the continental  
9 1151 crust and re-evaluation of fluxes in arcs. *Earth and Planetary Sciences Letters* 371-372:177-190.  
10 1152  
11 1153 Jagoutz O. 2014. Arc crustal differentiation mechanisms. *Earth and Planetary Science Letters*  
12 1154 396:267-77.  
13 1154  
14 1155  
15 1156 Jagoutz, O. and Kelemen, P.B., 2015, Role of arc processes in the formation of continental crust,  
16 1157 *Annual Reviews of Earth and Planetary Sciences*, 43:363-404.  
17 1157  
18 1158  
19 1159 Jan, M. Q. & Howie, R. A., 1981, The mineralogy and geochemistry of the metamorphosed basic  
20 1160 and ultrabasic rocks of the Jijal Complex, Kohistan, NW Pakistan. *Journal of Petrology* 22, 85-  
21 1161 126.  
22 1161  
23 1162  
24 1163 Jones CH, Reeg H, Zandt G, Gilbert H, Owens TJ, Stachnik J. 2014. P-wave tomography of  
25 1164 potential convective downwellings and their source regions, Sierra Nevada, California. *Geosphere*  
26 1165 10(3).  
27 1166  
28 1167 Jull, M., Kelemen, P., 2001. On the conditions for lower crustal convective instability.  
29 1167 *J. Geophys. Res.* 106, 6423–6446.  
30 1168  
31 1169  
32 1170 Kay, S. M., and Kay, R. W., 1985, Role of crystal cumulates and the oceanic crust in the formation  
33 1171 of the Aleutian arc: *Geology*, v. 13, p. 461-464  
34 1171  
35 1172  
36 1173 Kay R.W. and Kay S.M., 1993, Delamination and delamination magmatism, *Tectonophysics*,  
37 1174 219:177-189.  
38 1175  
39 1176 Kidder, S., Ducea, M., Gehrels, G., Patchett, P.J., Vervoort, J., 2003. Tectonic and magmatic  
40 1177 development of the Salinian Coast Ridge belt, California. *Tectonics* 22,  
41 1178 doi:10.1029/2002TC001409.  
42 1178  
43 1179  
44 1180 Kistler, R. W., 1990, Two different types of lithosphere in the Sierra Nevada, California, *Geol.*  
45 1181 *Soc. Am. Mem.*, v. 174, p. 271-282.  
46 1181  
47 1182  
48 1183 Klemperer, S., Hauge, T.A., Hauser, E.C., Oliver, J.E., Potter, C.J., 1986, The Moho in the  
49 1184 northern Basin and Range along the COCORP 40°N seismic reflection transect, *Geological Society*  
50 1185 *of America Bulletin*, 97, 603-618.  
51 1185  
52 1186  
53 1187 Laske, G., Masters, G., Ma, Z., Pasyanos, M., 2013. Update on CRUST1.0 – a 1-degree global  
54 1188 model of Earth’s crust. *Geophys. Res. Abstr.*, EGU2013-2658.  
55 1189  
56 1189  
57 1190 Lee, C-T, Yin, Q-Z, Rudnick, R L, Chesley, J T, Jacobsen, S B, 2000, Os isotopic evidence for  
58 1191 Mesozoic removal of lithospheric mantle beneath the Sierra Nevada, California, *Science* 289:  
59 1192 1912-1916.  
60  
61  
62  
63  
64  
65

- 1  
2  
3  
4 1193  
5 1194 Lee, C. T., Q. Z. Yin, R. L. Rudnick, and S. B. Jacobsen, 2001a, Preservation of ancient and fertile  
6 1195 lithospheric mantle beneath the southwestern United States, *Nature*, 411, 69-73.  
7 1196  
8 1196  
9 1197 Lee, C-T, Rudnick, R L, and Brimhall, G. H., Jr., 2001b, Deep lithospheric dynamics beneath the  
10 1198 Sierra Nevada during the Mesozoic and Cenozoic as inferred from xenolith petrology,  
11 1199 *Geochemistry Geophysics Geosystems* 2, 2001GC000152.  
12 1200  
13 1200  
14 1201 Lee, C.-T., Cheng, X., Horodyskyj, 2006. The development and refinement of continental arcs by  
15 1202 primary basalt magmatism, garnet pyroxenite accumulation, basaltic recharge and delamination:  
16 1203 insights from the Sierra Nevada, California. *Contrib. Mineral. Petrol.* 151, 222–242.  
17 1204  
18 1204  
19 1205 Lee, C.-T.A., 2014. Physics and chemistry of deep continental crust recycling. In: Holland, H.,  
20 1206 Turekian, K. (Eds.), *Treatise of Geochemistry*, 2nd ed. Elsevier, pp.423–456.  
21 1207  
22 1207  
23 1208 Lee, C-T A and Anderson, D., 2015, Continental crust formation at arcs, the arclogite  
24 1209 “delamination” cycle, and one origin for fertile melting anomalies in the mantle, *Science Bulletin*  
25 1210 DOI:10.1007/s11434-015-0828-6  
26 1211  
27 1212 Mamani M, Wörner G, Sempere T. , 2010, Geochemical variations in igneous rocks of the Central  
28 1213 Andean orocline (13°S to 18°S): Tracing crustal thickening and magma generation through time.  
29 1214 *Geological Society of America Bulletin* 122:162–82.  
30 1214  
31 1215  
32 1216 McInnes, B.I.A., Gregoire, M., Binns, R.A., Hannington, M.D., 2001, Hydrous metasomatism of  
33 1217 oceanic sub-arc mantle, Lihir, Papua New Guinea: Petrology and geochemistry of fluid-  
34 1218 metasomatised mantle wedge xenoliths, *Earth and Planetary Sciences Letters*, 188, 169-183.  
35 1218  
36 1219  
37 1220 Meissner, R., *The Continental Crust: A Geophysical Approach*, Academic, San Diego, Calif.,  
38 1221 1986.  
39 1221  
40 1222  
41 1223 Mukhopadhyay, B., 1989, Petrology and geochemistry of mafic and ultramafic xenoliths from  
42 1224 the Sierra Nevada batholith, Part 1, PhD dissertation, Univ. Texas Dallas, 215 p.  
43 1225  
44 1226 Mukhopadyay B., Manton W.I. 1994, Upper mantle fragments from beneath the Sierra Nevada  
45 1227 batholith: Partial fusion, fractional crystallization and metasomatism in a subduction-enriched  
46 1228 ancient lithosphere, *Journal of Petrology*, 35: 1418-1450.  
47 1228  
48 1229  
49 1230 Murphy, M. and Chapman, A.D., 2018, Rooting around beneath an arc: Zircon U-Pb  
50 1231 geochronologic and Hf isotopic constraints on the evolution of the base of the Sierra Nevada  
51 1232 batholith. Abstracts with programs - Geological Society of America, 50(6).  
52 1232  
53 1233  
54 1234 Nakamura, D., 2009, A new formulation of garnet–clinopyroxene geothermometer based on  
55 1235 accumulation and statistical analysis of a large experimental data set. *Journal of Metamorphic*  
56 1236 *Geology*, 27: 495-508. doi:10.1111/j.1525-1314.2009.00828.x  
57 1236  
58 1237  
59  
60  
61  
62  
63  
64  
65

- 1  
2  
3  
41238 Newton, R.C. and D . Perkins, III, Thermodynamic calibra. tion of geobarometer based on the  
51239 assemblages garnet- plagioclase-orthopyroxene (cpx)-quartz, *Am. Mineral.* 67, 203- 222, 1982  
61240  
71241 Nixon, P.H. 1987, *Mantle xenoliths*. Wiley, United States: 884 p, ISBN-13: 978-0471912095.  
81242  
91243 Obata, M., 1980, The Ronda peridotite: garnet-, spinel-, and plagioclase-lherzolite facies and the  
101244 P-T trajectories of a high- temperature mantle intrusion. *Journal of Petrology* 21, 533-572.  
111244  
121245  
131246 Otamendi, J.E., Ducea, M.N., Tibaldi, A.M., Bergantz, G.W., de la Rosa, J.D., Vujovich, G.I.,  
141247 2009. Generation of tonalitic and dioritic magmas by coupled partial melting of gabbroic and  
151248 metasedimentary rocks within the deep crust of the Famatinian magmatic arc, Argentina. *Journal*  
161248 of *Petrology* 50, 841-873.  
171249  
181250  
191251 Otamendi, J.E., Ducea, M.N., Bergantz, G.W., 2012. Geological, petrological and geochemical  
201251 evidence for progressive construction of an arc crustal section, Sierra de Valle Fertil, Famatinian  
211252 Arc, Argentina. *Journal of Petrology* 53, 761-800.  
221253  
231254  
241255 Paterson, S.R., Farris, D.W., 2008. Downward host rock transport and the formation of  
251255 rimmonoclines during the emplacement of Cordilleran batholiths. *Transactions of the Royal*  
261256 *Society of Edinburgh: Earth Sciences* 97 (n. 4), 397–413 (Special Issue *Plutons and Batholiths*  
271257 (The Wallace Pitcher Memorial Volume)).  
281258  
291259  
301260  
311261  
321261 Pearson, D. G., Davies, G. R. & Nixon, P. H. , 1993, Geochemical constraints on the petrogenesis  
331262 of diamond facies pyroxenites from the Beni Bousera peridotite massif, North Morocco. *Journal*  
341262 of *Petrology*, 34, 125-172.  
351263  
361264  
371265 Perkins, D., III, and R. C. Newton, 1981, Charnockite geobarometers based on coexisting garnet-  
381266 plagioclase-pyroxene-quartz, *Nature*, 292, 144-146.  
391267  
401268 Petermann, M., Hirschmann, M., 2003. Partial melting experiments on a MORB- like  
411268 pyroxenite between 2 and 3 GPa: constraints on the presence of pyroxenite in basalt source  
421269 regions from solidus location and melting rate. *J. Geophys. Res.* 108, 2125.  
431270  
441271  
451272 Philpotts, A., Ague, J., 2009. *Principles of igneous and metamorphic petrology*. Cambridge  
461272 University Press.  
471273  
481274  
491275 Pickett D.A. and Saleeby J.B., 1993, Thermobarometric constraints on the depth of exposure and  
501276 conditions of plutonism and metamorphism at deep levels of the Sierra Nevada batholith,  
511276 Tehachapi Mountains, California, *J. Geophys. Res.*, 98: 609-629.  
521277  
531278  
541279 Profeta, L., Ducea, M.N., Chapman, J.B., Paterson, S.R., Gonzales, S.M.H., Kirsch, M., Petrescu,  
551280 L., DeCelles, P.G., 2015. Quantifying crustal thickness over time in magmatic arcs. *Scientific*  
561281 *Reports* 5, 17786, doi:10.1038/srep17786.  
571281  
581282  
591283 Rapp R.P., Watson E.B., 1995. Dehydration melting of metabasalt at 8-32 kbar; implications for  
60  
61  
62  
63  
64  
65

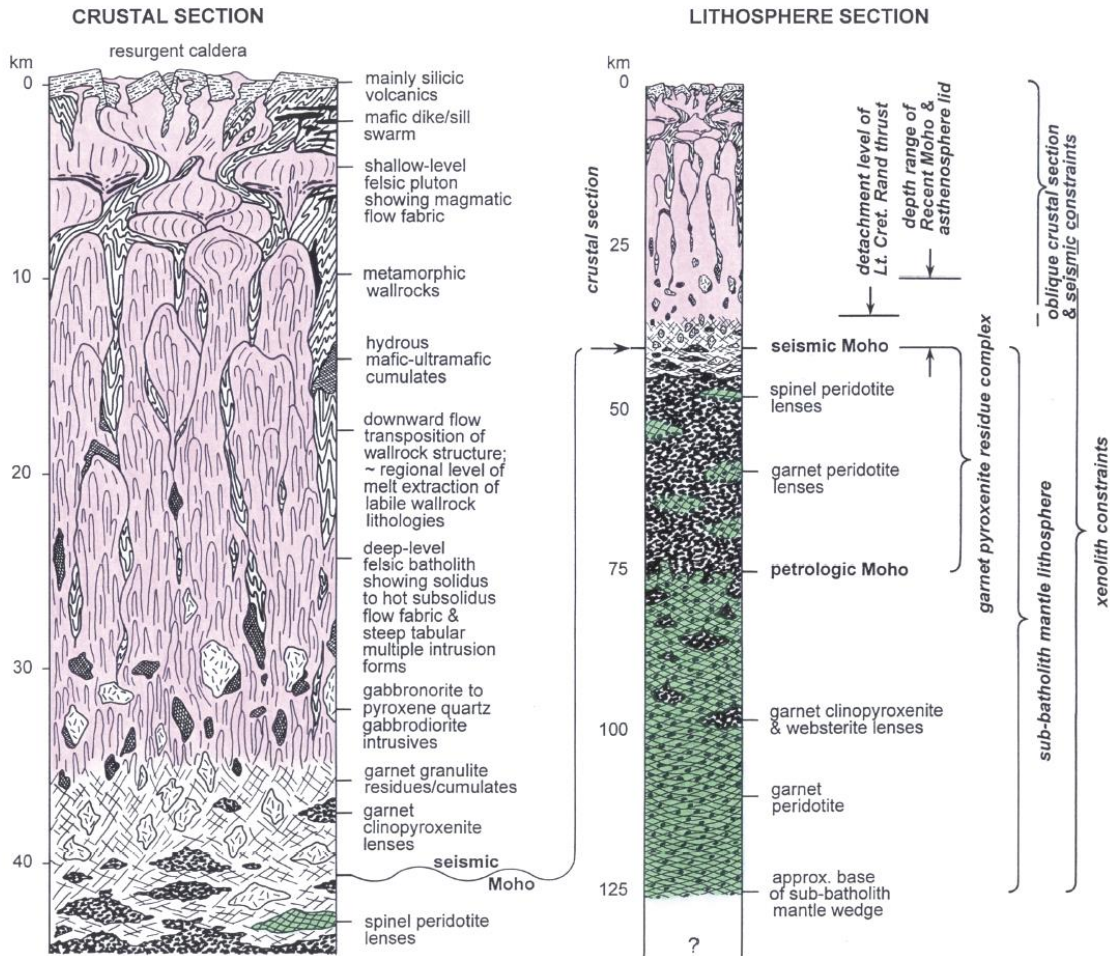
1  
2  
3  
4 1284 continental growth and crust-mantle recycling. *Journal of Petrology* 36:891-931.  
5  
6 1285  
7 1286 Rautela, O., Chapman, A.D., Shields, J.E., Ducea, M.N., Lee, C.-T., Jiang, H., and Saleeby, J., in  
8 1287 press, In search for the missing arc root of the Southern California Batholith: P-T-t evolution of  
9 1288 upper mantle xenoliths of the Colorado Plateau Transition Zone, *Earth and Planetary Science*  
10 1289 *Letters*.  
11  
12 1290  
13 1291 Rodriguez-Vargas, A., Koester, E., Mallmann, G., Conceição, R., Kawashita, K., We- ber, M.,  
14 1292 2005. Mantle diversity beneath the Colombian Andes, Northern Volcanic Zone: constraints from  
15 1293 Sr and Nd isotopes. *Lithos* 82, 471–484.  
16  
17 1294  
18 1295 Rudnick, R. L., Barth, M., Horn, I. & McDonough, W. F. 2000, Rutile-bearing refractory eclogites:  
19 1296 missing link between continents and depleted mantle. *Science* 287, 278–281.  
20 1297  
21 1298 Rudnick, R., 1995. Making continental crust. *Nature* 378, 571–578.  
22  
23 1299  
24 1300 Rushmer, T., 1991, Partial melting of two amphibolites: contrasting experimental results under  
25 1301 fluid-absent conditions, *Contributions to Mineralogy and Petrology*, 107, 41-59.  
26 1302  
27 1303 Saleeby, J.B., 1990. Progress in tectonic and petrogenetic studies in an exposed cross-section of  
28 1304 young (~100 Ma) continental crust, southern Sierra Nevada, California. In: Salisbury, M.H. (Ed.),  
29 1305 *Exposed Cross Sections of the Continental Crust*. D.Reidel Publishing, Dordrecht, pp. 132–158.  
30 1306  
31 1307  
32 1308 Saleeby, J. B., M. N. Ducea, and D. Clemens-Knott, 2003, Production and loss of high-density  
33 1309 batholithic root, southern Sierra Nevada, California, *Tectonics*, 22, doi: 10.1029/2002TC001374.  
34 1310  
35 1311  
36 1312 Saleeby, J., 2003. Segmentation of the Laramide slab: evidence from the southern Sierra Nevada  
37 1313 region. *Geological Society of America Bulletin* 115, 655–668.  
38 1314  
39 1315 Schmidt, M. W., and O. Jagoutz, 2017, The global systematics of primitive arc melts,  
40 1316 *Geochemistry Geophysics Geosystems*, 18, 817–2854, doi:10.1002/2016GC006699  
41 1317  
42 1318  
43 1319 Smith, D., Arculus, R.J., Manchester, J.E., and Tyner, G.N., 1994, Garnet-pyroxene-amphibole  
44 1320 xenoliths from Chino Valley, Arizona, and implications for continental lithosphere below the  
45 1321 Moho, *Journal of Geophysical Research*, v. 99, n. B1, p. 683-696.  
46 1322  
47 1323  
48 1324 Stern RJ. 2002. Subduction zones. *Reviews of Geophysics* 40:4-34.  
49 1325  
50 1326  
51 1327 Sun, c., Liang, y. (2015) A REE-in-garnet-clinopyroxene thermobarometer for eclogites,  
52 1328 granulites and garnet peridotites. *Chemical Geology* 393-394, 79-92  
53 1329  
54 1330  
55 1331 Tang, M., Lee, C.-T. A., Chen, K., Erdman, M., Costin, G., & Jiang, H. (2019). Nb/Ta systematics  
56 1332 in arc magma differentiation and the role of arclogites in continent formation. *Nature*  
57 1333 *Communications*, 10, <https://doi.org/10.1038/s41467-018-08198-3>.  
58 1334  
59  
60  
61  
62  
63  
64  
65

- 1  
2  
3  
4 1329 Tassara, A., Swain, C., Hackney, R., Kirby, J., 2007. Elastic thickness structure of South America  
5 1330 estimated using wavelets and satellite-derived gravity data. *Earth and Planetary Science Letters*  
6 1331 253, 17–36 <http://dx.doi.org/10.1016/j.epsl.2006.10.008>.  
8 1332
- 9 1333 Tatsumi Y. 2000. Continental crust formation by crustal delamination in subduction zones and  
10 1334 complementary accumulation of the enriched mantle I component in the mantle. *Geochem.*  
11 1335 *Geophys. Geosyst.* 1:1053  
13 1336
- 14 1337 Tatsumi, Y., 2005, The subduction factory: how it operates in the evolving Earth, *GSA Today* 15,  
15 1338 4-10.  
16 1339
- 17 1340 Taylor S. R., McLennan S.M., 1985, *The continental crust; Its compositional evolution*, Blackwell  
18 1341 *Sci.*, Cambridge, Mass, 312p.  
20 1342
- 21 1343 Vielzeuf, D., and M. W. Schmidt, Melting relations in hydrous systems revisited: Application to  
22 1344 metapelites, metagraywackes and metabasalts, *Contrib. Mineral. Petrol.*, 141, 251–267, 2001.  
24 1345
- 25 1346 Walker Jr, B.A., Bergantz, G.W., Otamendi, J.E., Ducea, M.N., Cristofolini, E.A., 2015. A MASH  
26 1347 zone revealed: the mafic complex of the Sierra Valle Fértil. *Journal of Petrology* 56, 1863-1896.  
27 1348
- 28 1349 Ward, K.M., Delph, J.R., Zandt, G., Beck, S.L., Ducea, M.N., 2017. Magmatic evolution of a  
30 1350 Cordilleran flare-up and its role in the creation of silicic crust, *Scientific Reports* 7, 9047,  
31 1351 doi:10.1038/s41598-017-09015-5.  
32 1352
- 33 1353 Watson, E. B., Wark, D. A., and Thomas, J. B., 2006, Crystallization thermometers for zircon and  
34 1354 rutile, *Contributions to Mineralogy and Petrology*, 151, 413-433.  
36 1355
- 37 1356 Weber, M., Tarney, J., Kempton, P., Kent, R., 2002. Crustal make-up of the northern Andes:  
38 1357 evidence based on deep crustal xenolith suites, Mercaderes, SW Colombia, *Tectonophysics*  
39 1358 345, 49–82.  
40 1359
- 41 1360 Wendlandt, E., DePaolo, D.J., and Baldrige, W.S., 1996, Thermal history of Colorado Plateau  
43 1361 lithosphere from Sm-Nd mineral geochronology on xenolith, *Geol. Soc. Am. Bull.*, v. 108, p. 757-  
44 1362 767.  
45 1363
- 46 1364 Wernicke, B., and Getty, S.R., 1997, Intracrustal subduction and gravity currents in the deep crust:  
48 1365 Sm-Nd, Ar-Ar, and thermobarometric constraints from the Skagit Gneiss Complex, Washington:  
49 1366 *Geological Society of America Bulletin*, v. 109, p. 1149-1166.  
50 1367
- 51 1368 Wernicke B., and 19 others (1996) Origin of high mountains on continents: The Southern Sierra  
53 1369 Nevada, *Science*, 271: 190-193.  
54 1370
- 55 1371 Whitney, D.L., 1992, Origin of CO<sub>2</sub>-rich fluid inclusions in leucosomes from the Skagit  
56 1372 migmatites, North Cascades, Washington, USA: *Journal of Metamorphic Geology*, v. 10, p. 715-  
58 1373 725.  
59 1374

1  
2  
3  
41375 Wolf M.B., and Wyllie P.J., 1993, Garnet growth during amphibolite anatexis: Implications for a  
51376 garnetiferous restite, *J. Geol.*, 101:357-373.  
61377  
71378 Wolf MB, and Wyllie PJ. 1994. Dehydration-melting of amphibolite at 10 kbar; the effects of  
81379 temperature and time. *Contributions to Mineralogy and Petrology* 115:369-83.  
91380  
101381 Yamamoto, H. & Nakamura, E., 1996, Sm-Nd dating of garnet granulites from the Kohistan  
111382 Complex, northern Pakistan. *Journal of the Geological Society, London* 153, 965-969.  
121383  
131384 Yamamoto, H. & Nakamura, E. , 2000, Timing of magmatic and metamorphic events in the Jijal  
141385 Complex of the Kohistan Arc deduced from Sm-Nd dating of mafic granulites. *Geological Society,*  
151386 *London, Special Publications* 170, 313-319.  
161387  
171388 Yuan, X., Sobolev, S.V., Kind, R., 2002. Moho topography in the central Andes and its  
181389 geodynamic implications. *Earth Planetary Science Letters* 199, 389–402 [http://](http://dx.doi.org/10.1016/S0012-821X(02)00589-7)  
191390 [dx.doi.org/10.1016/S0012-821X\(02\)00589-7](http://dx.doi.org/10.1016/S0012-821X(02)00589-7).  
201391  
211392 Zandt, G., Gilbert, H., Owens, T., Ducea, M., and Saleeby, J., 2004. Active foundering of  
221393 a continental arc root beneath the southern Sierra Nevada in California. *Nature* 431, 41–46.  
231394  
241395 Zeilinger, G., 2002, Structural and geochronological study of the lowest Kohistan Complex, Indus  
251396 Kohistan region in Pakistan, NW Himalaya. PhD thesis, ETH, Zurich.  
261397  
271398 Zindler, A., Hart, S., 1986, Chemical geodynamics. *Annual Review of Earth and Planetary*  
281399 *Sciences*, 14, 493–571.  
291400  
301401  
311402  
32  
33  
34  
35  
36  
37  
38  
39  
40  
41  
42  
43  
44  
45  
46  
47  
48  
49  
50  
51  
52  
53  
54  
55  
56  
57  
58  
59  
60  
61  
62  
63  
64  
65



1  
2  
3  
4 1403 **Figures**  
5  
6  
7  
8  
9



42 1404  
43  
44 1405 **Figure 1.** Schematic vertical composition of the lithosphere beneath a Cordilleran arc (modified  
45 after Saleeby et al., 2003), as revealed by the Sierra Nevada exposures (0-30 km paleodepths) and  
46 1406 various post batholithic xenolith localities described in text. The lithosphere is about 125 km thick  
47 1407 and is characterized by a significantly different depth to petrologic and seismic Moho, given the  
48 1408 abundance of ultramafic residues. Rocks referred to as “garnet clinopyroxenites” in this figure by  
49 1409 Saleeby et al. (2003) and most other researchers at the time, are now renamed arclogites.  
50  
51 1410  
52  
53 1411

54  
55 1411  
56  
57  
58  
59  
60  
61  
62  
63  
64  
65

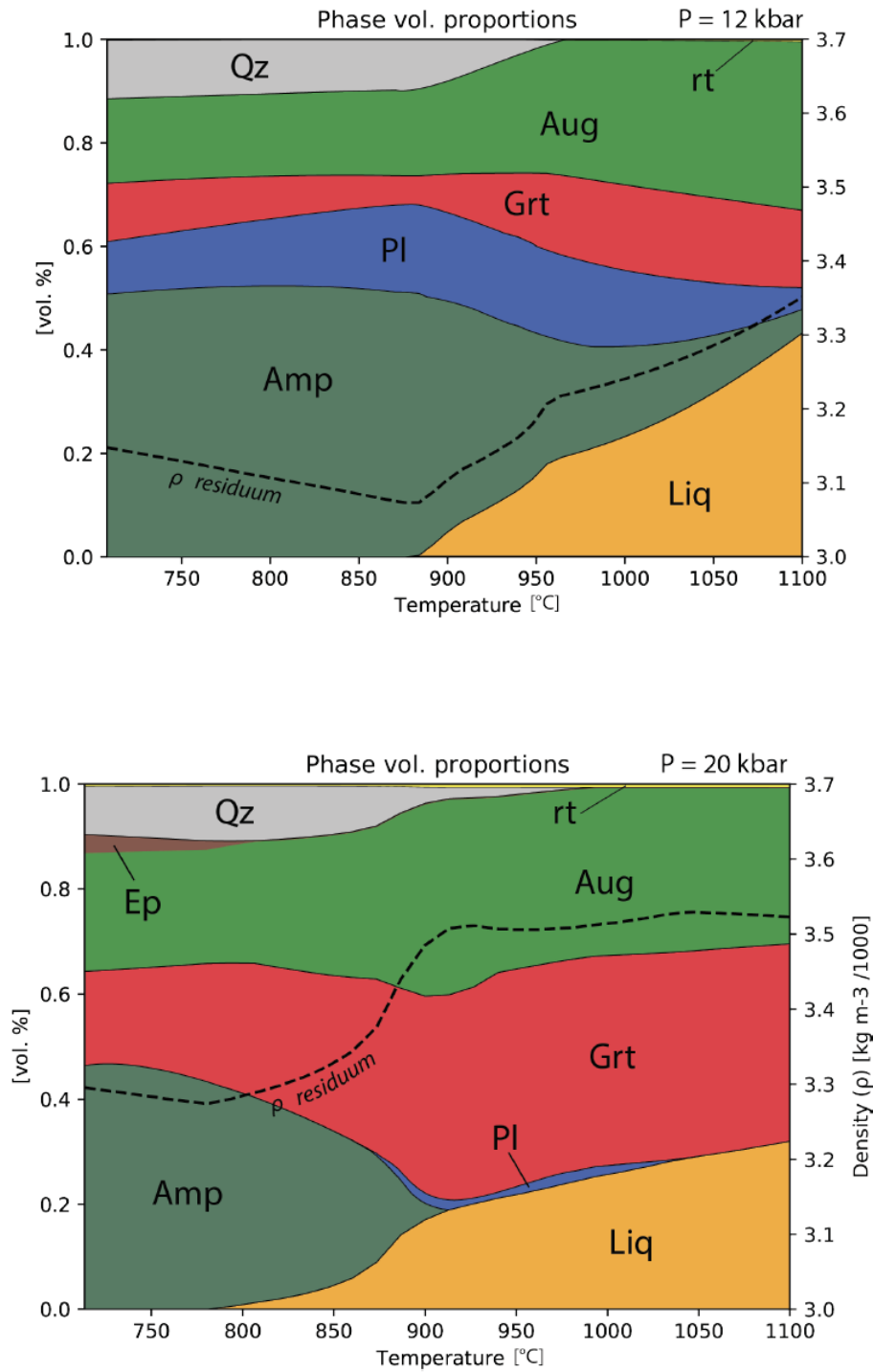
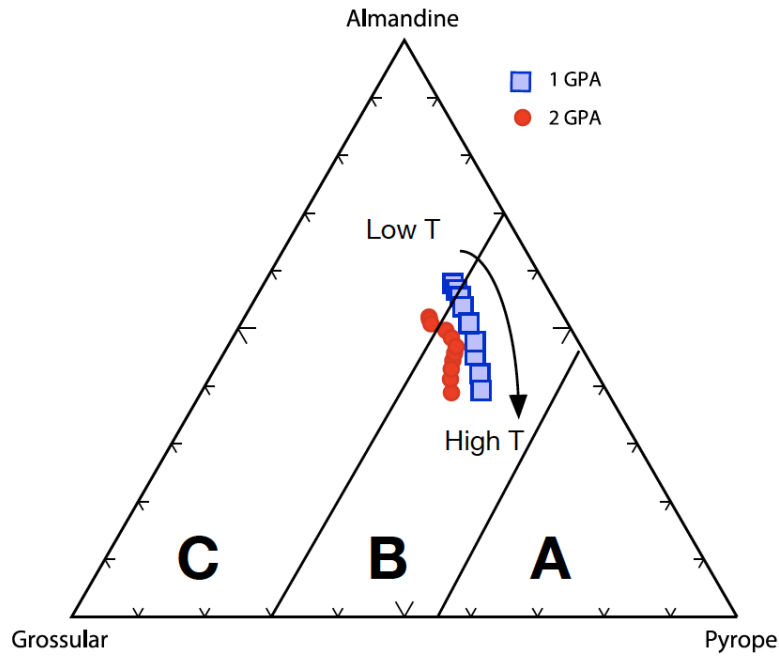


**Figure 2.** Experimental prediction of garnet, plagioclase, amphibole and other phases on the liquidus of an intermediate melt and below the solidus for an average arc basalt starting

composition (with 4% water). Phases are shown at 1.2 GPa (panel above) and 2 GPa (panel below). Density of the residual phases are shown on the right in  $g/cm^3$ . Calculated using deCapitani & Petrakakis (2010). Abbreviations: Qz-quartz, Amp-amphibole, Pl- Plagioclase, Ep-Epidote, Rt-rutile, Grt-garnet, Aug-Augite, Liq-liquid.



Coleman et al., 1965

**Figure 3.** Predicted garnet compositions for the fractionation of an intermediate magma at 1 and 2 GPa, using pMELTS (Ghiorso and Sack, 1995). Starting material is an average arc basalt (Schmidt and Jagoutz, 2017). The ternary classification diagram for garnets is from Coleman et al. (1965).



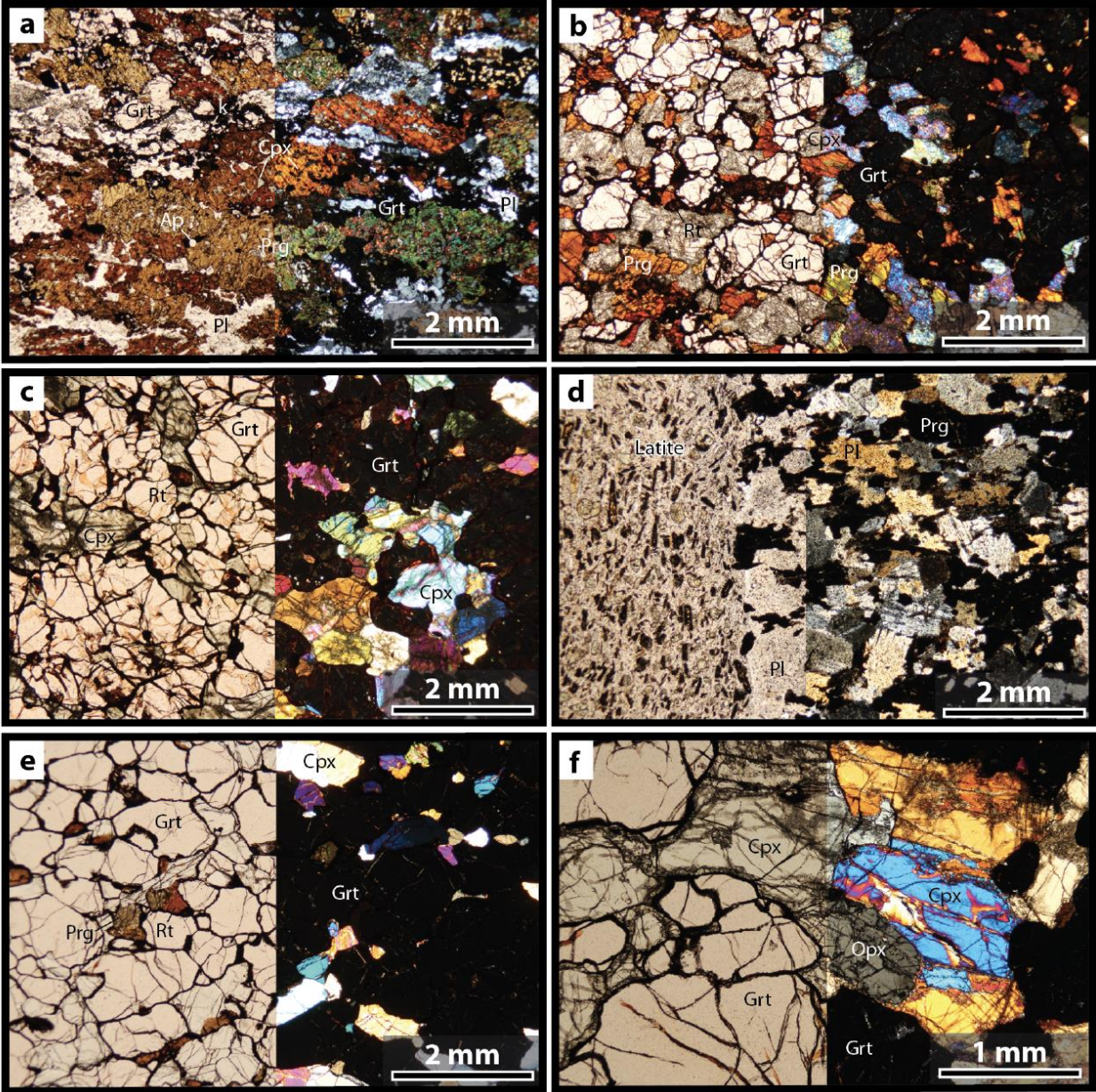


**Figure 4.** Photomicrographs of petrologic features in Central Arizona localities: arclogites and related xenoliths (from Chapman et al., 2019). All panels show plane-polarized light on the left and cross-polarized light on the right, respectively. (A) Camp Creek garnet clinopyroxenite (group 1) with relict clinopyroxene in cores of amphibole, which has replaced most of the primary clinopyroxene. Note plagioclase-rich injected melt pockets, kelyphitized garnet rim domains, and moderately strong foliation defined by elongate amphibole running from left to right of frame. (B) Camp Creek arclogite with a higher proportion of primary clinopyroxene to secondary amphibole than sample shown in A. (C) Equigranular Camp Creek fresh arclogite.

(D) Chino Valley amphibolitized felsic granulite gneiss. Note biotite-clinopyroxene latite showing flow foliation from top to bottom of photo. (E) Chino Valley fresh arclogite with minor secondary pargasitic amphibole replacing clinopyroxene (group 2). (F) Chino Valley fresh garnet-websterite. Sample yields Late Jurassic garnet-whole rock isochron age. Mineral abbreviations: Ap—apatite; Krs—kaersutitic amphibole; Cpx—clinopyroxene; Grt—garnet; Ilm—ilmenite; K—kelyphite; Opx—orthopyroxene; Prg—pargasitic amphibole; Pl—plagioclase; Rt—rutile.

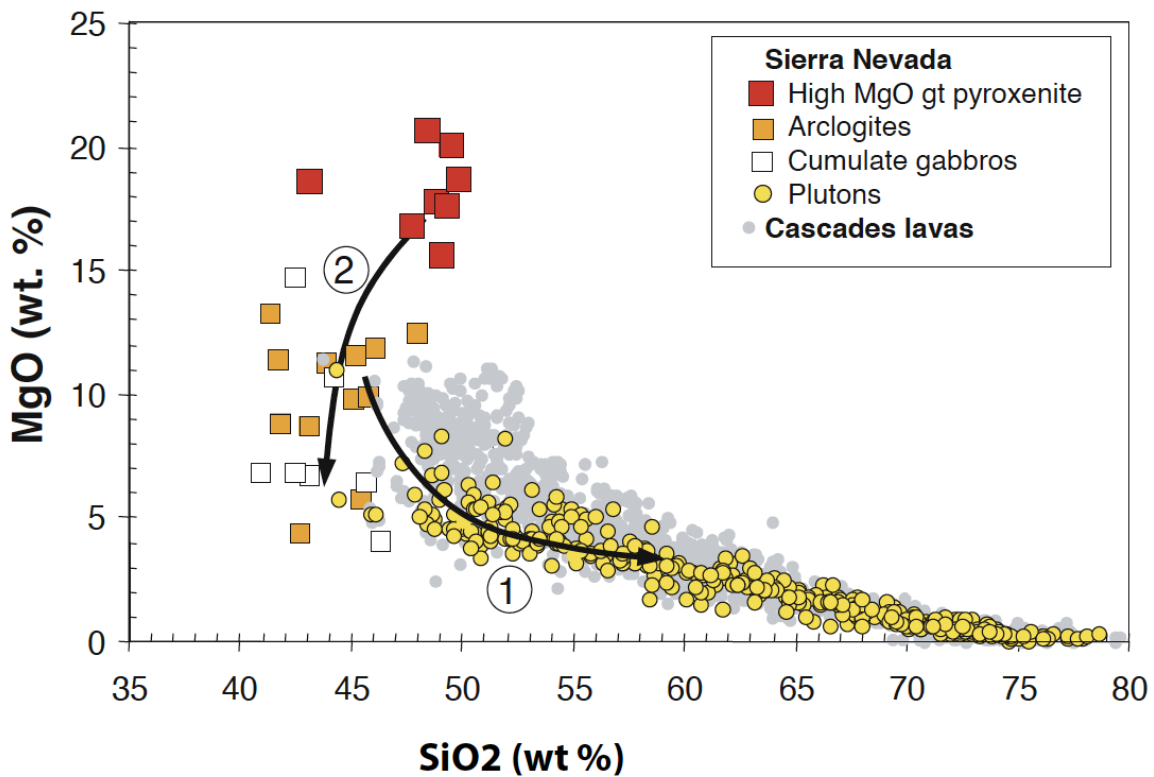


**Figure 5.** Harker diagram showing compositional trends of two major arcs (plutons from the Sierra Nevada and volcanic rocks from the modern Cascades) (trend 1) and the opposite trend (2) typical for cumulate and restites of the Sierra Nevada (modified from Lee et al., 2006). This trend is identical to those seen in other studies (see Ducea, 2002 for example). High Mg garnet pyroxenites here are high pressure (mantle-derived) garnet westeritic assemblages (see text for details).

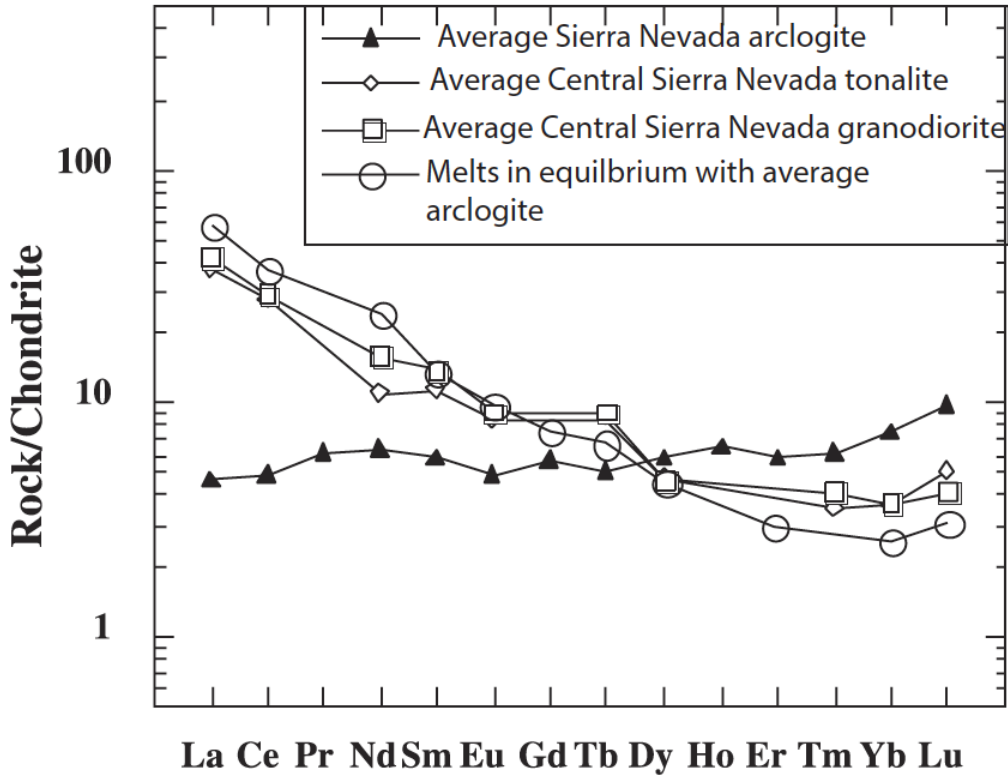


**Figure 6.** Rare earth elemental chemistry of average Sierra Nevada arclogite (Ducea, 2002), calculated melts in equilibrium with that residue (using partition coefficients listed in Ducea, 2002), as well as average composition of the main lithologic types in the central Sierra Nevada batholith, tonalites and granodiorites (numerous sources compiled in NAVDAT.org).



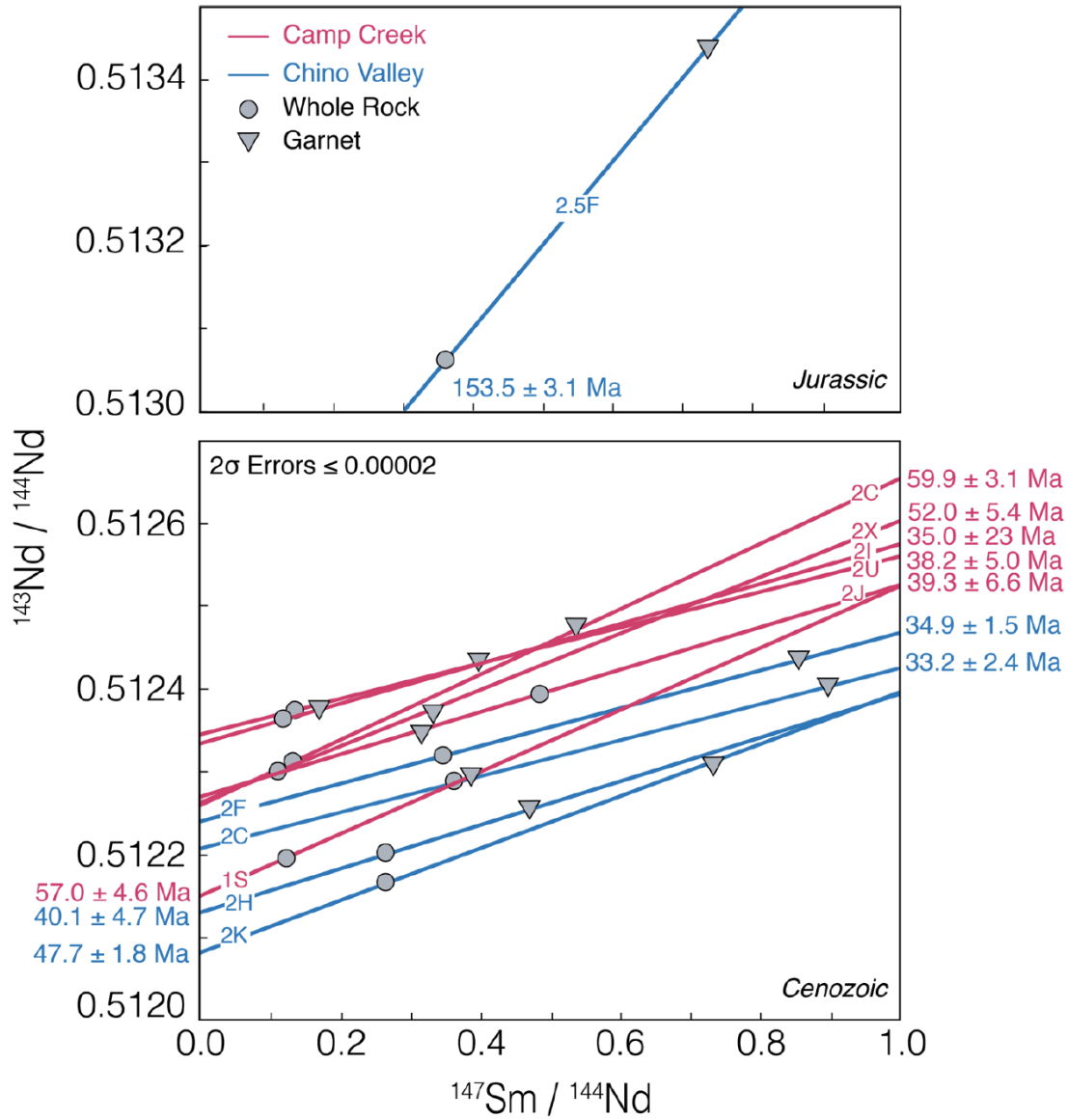


**Figure 7.** Sm-Nd garnet-whole rock geochronology for the central Arizona arclogites. One Chino Valley sample 16CV2.5F records a Jurassic age. Remaining samples yield Late Cretaceous – Early Cenozoic ages, suggesting partial re-equilibration of the samples with host latite (Chapman et al. 2019, Rautela et al, 2020)

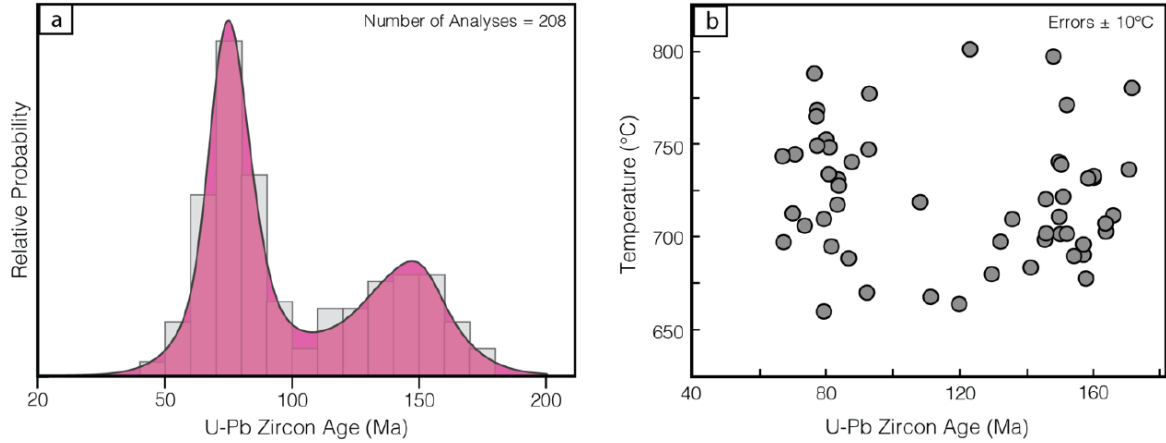


**Figure 8.** Zircon U-Pb age distribution and Ti-in-zircon thermometry trend over time for the central Arizona arclogites (from Chapman et al., 2019, 2020 and Rautela et al., 2020). (a) A probability density diagram of U-Pb zircon ages of the samples (data from Chapman et al., 2020). Note two age peaks at ca. 150 Ma and ca. 70 Ma. (b) Ti-in-zircon thermometry (Watson et al., 2006) showing elevated temperatures (>650 C) from Jurassic through Cenozoic time.



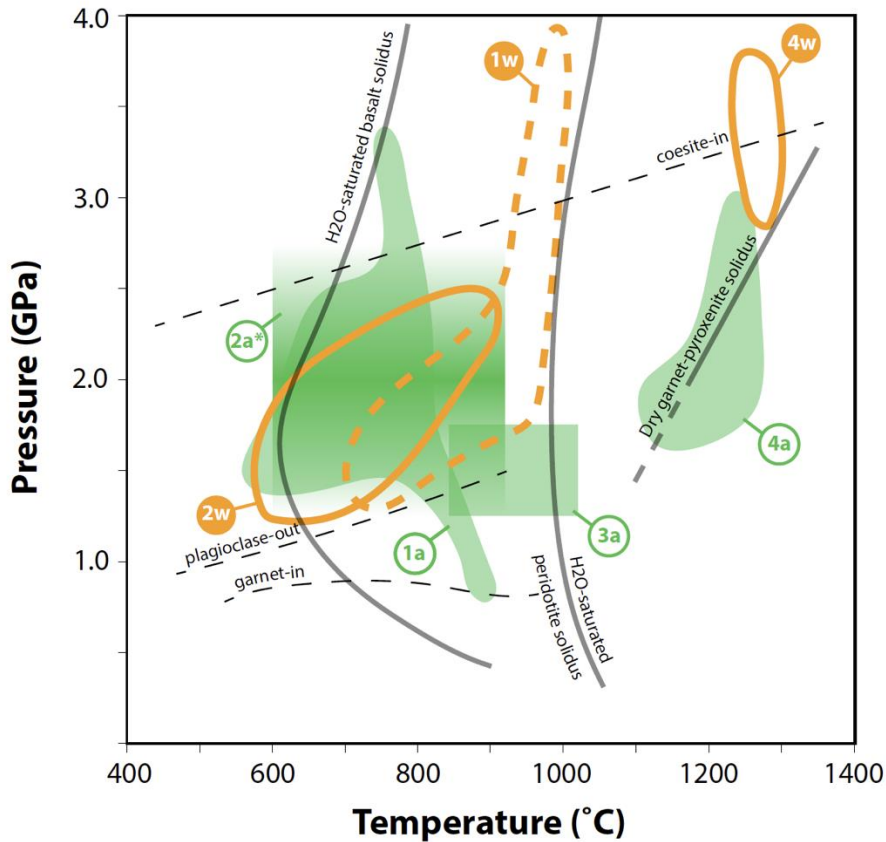


**Figure 9.** Summary of pressure-temperature constraints available from arclogite (labeled “a” in green filled fields) plus garnet websterite and garnet peridotite (combined and labeled “w” in fields with orange outlines) xenoliths. Fields 1-4 contain data from central Sierra Nevada (California; Mukhopadhyay and Manton, 1994; Ducea and Saleeby, 1996; Lee et al., 2000, 2001, 2006; Chin et al., 2015), central Arizona (Esperanca et al., 1988; Smith et al., 1994; Erdman et al., 2016; Rautela et al., 2020), Beni Bousera (Morocco; Gysi et al., 2011), and Mercaderes (Colombia; Bloch et al., 2017) localities, respectively. Plagioclase-out and garnet-in isograds from Wolf and Wyllie (1993, 1994), Hydrous basalt and peridotite solidi from Rapp and Watson (1995) and Vielzeuf and Schmidt (2001), dry garnet clinopyroxenite solidus and low P-T projection (dashed) from Petermann and Hirschmann (2003). \*Temperatures calculated at 2.0 GPa (garnet-orthopyroxene thermobarometry on websterite xenoliths from Chino Valley). A minimum pressure constraint of 0.9 GPa on central Arizona garnet clinopyroxenite is provided by garnet-plagioclase-orthopyroxene-quartz barometry on granulite xenoliths from Camp Creek.

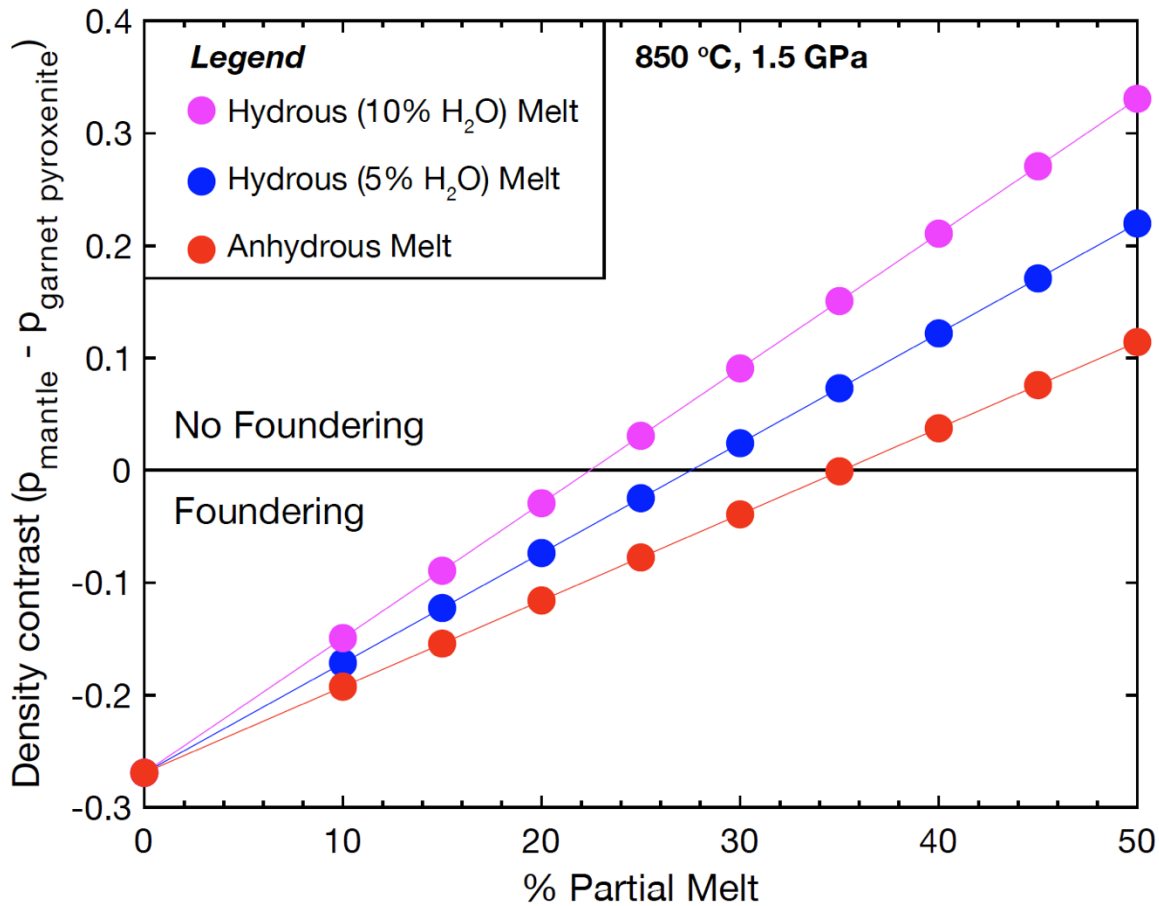


**Figure 10.** Diagram showing the density contrast between typical upper mantle peridotite and arclogite at 850 °C and 1.5 GPa, with various fractions of intermediate partial melt for anhydrous melt, 5% H<sub>2</sub>O and 10% H<sub>2</sub>O. If density contrast is positive (root denser than melt), foundering is possible, otherwise not. Diagram shows that if percentage of partial melt is >22-35% , arclogitic roots are not gravitationally unstable. Average arclogitic compositions from Ducea (2002) Lee et al. (2006) was used here. Density calculated with a modified version of Hacker and Abers (2016).

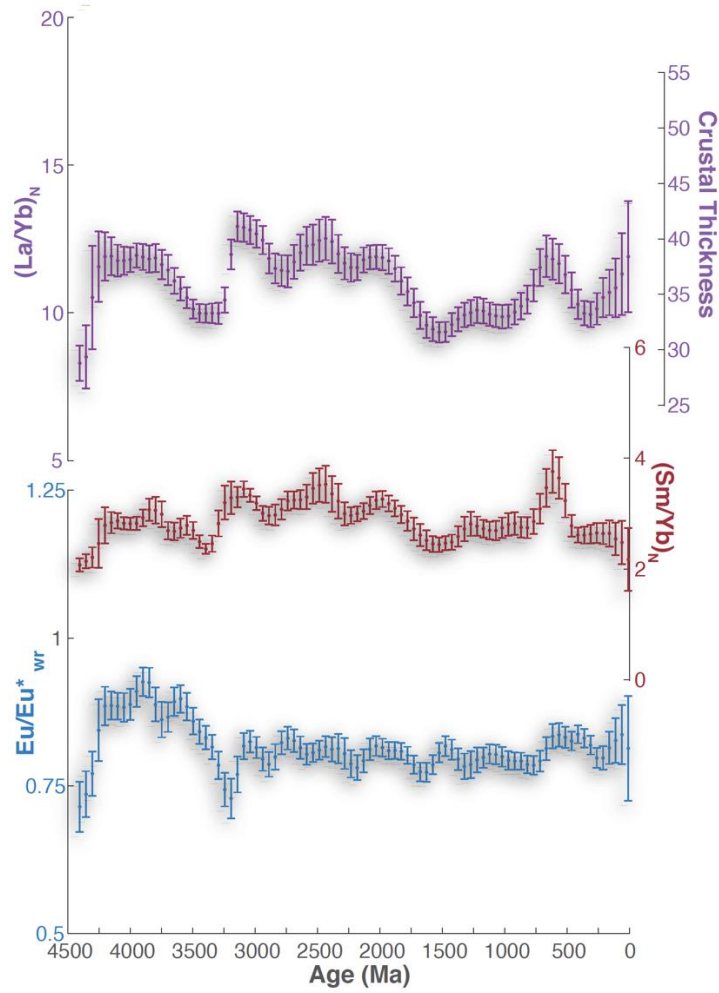


**Figure 11.** Global calculated whole rock  $La/Yb_n$ ,  $Sm/Yb_n$  and  $Eu/Eu^*$  from zircon petrochronology (Balica et al., 2020). Crustal thickness over time is also shown on the right (as determined by Profeta et al., 2015 based on  $La/Yb$ ). 98% all analyzed zircons are from granitoid magmas (Balica et al., 2020). Diagram shows that to a first order, granitoids were fractionated out of magmatic systems at 35-45 km over time, similar to conditions required to make arclogitic roots. Mechanisms for fractionating or remelting basalts under lower crustal conditions may however have been different in the geologic past compared to modern arc settings (Balica et al., 2020).